A Systematic Review on Medical Image Segmentation using Deep Learning

Mahdiyeh Rahmani [a, b], Ali Kazemi [a, b], Maryam Jalili Aziz [c], Ebrahim Najafzadeh [d], Parastoo Farnia [a, b, *], Alireza Ahmadian [a, b, *]

[a] *Medical Physics and Biomedical Engineering Department, Faculty of Medicine, Tehran University of Medical Sciences (TUMS), Tehran, Iran.*

[b] *Research Center of Biomedical Technology and Robotics (RCBTR), Advanced Medical Technologies & Equipment Institute (AMTEI), Imam Khomeini Hospital Complex, Tehran University of Medical Sciences (*

TUMS), Tehran, Iran.

[c] *Department of Electronic and Informatics, Vrije Universities Brussel, Brussels, Belgium, IMEC, Kapeldreef 75, 3001 Leuven, Belgium.*

[d] *Department of Medical Physics, School of Medicine, Iran University of Medical Sciences (IUMS), Tehran, Iran.*

* Corresponding author. Tel.: +982166482655

E-mail addresses: rahmanimahdiye@gmail.com (Mahdiyeh Rahmani)

301kazemi@gmail.com (Ali Kazemi)

jaliliazizmaryam@gmail.com (Maryam Jalili Aziz)

ebrahim.najafzadeh@gmail.com (Ebrahim Najafzadeh)

p-farnia@sina.tums.ac.ir (Parastoo Farnia)

ahmadian@sina.tums.ac.ir (Alireza Ahmadian)

A Systematic Review on Medical Image Segmentation Using Deep Learning

Abstract:

Medical image segmentation is an essential step in various diagnostic and treatment procedures. This study aimed to conduct a systematic review of state-of-the-art segmentation methods based on the target. The target complexity is a considerable challenge in medical image segmentation and the first issue that experts confront in diagnosing or treating patients. Additionally, each group of targets has similar characteristics, motivating to provide a target-based review to compare the deep-learning (DL)-based studies. This is the first time that a target-based review of medical image segmentation has provided a focus on recent DL developments. This study categorized publications into three targets: tumors, vessels, and pathological. Using a PRISMA strategy while considering the inclusion and exclusion criteria, 118 articles were identified on Google Scholar and PubMed from 2015 to 2023 in the fields of brain, liver, and lung tumors, blood vessels, and pathology image segmentation. This review could assist researchers in selecting the proper network and being aware of possible challenges. We also concluded that medical image segmentation using DL as a cross-disciplinary field is involved with both complex medical data and technical issues. Consequently, new interpretable approaches may be able to bridge the gap between medical specialists and artificial intelligence researchers.

Keywords: Medical image segmentation, deep learning, tumor segmentation, vessel segmentation, pathological image segmentation, target-based review.

1. Introduction

Over the last decade, medical image segmentation has been extensively investigated and has played a crucial role in computer-aided diagnostic systems. It is considered an essential step in medical image analysis in order to assist the clinician in conducting an accurate diagnosis and treatment. Image segmentation is the process of dividing an image into several disjointed areas based on features such as grayscale, spatial texture, and geometric shapes, along with a specific description [1]. The most popular medical image segmentation studies involve segmenting various elements, such as cells, tumors within different tissues (such as the cardiac, brain, liver, and lungs), the optic disc, pulmonary nodules, blood vessels, etc. [2].

Image segmentation methods could be classified into three categories in proportion to the degree of human interaction, including manual, semi-automatic, and automatic segmentation. Manual segmentation is done by an expert, a specialist radiologist, or a clinician. Therefore, it would serve as the ground truth to evaluate any segmentation method. On the other hand, manual segmentation

is prone to a great deal of variation, which may give rise to expert conflicts and is a time-consuming and laborious process.

Semi-automatic segmentation tries to address some problems associated with manual segmentation using algorithms such as growing segmentation in one re or expanding segmentation to other sections to eliminate the need for slice-by-slice segmentation, which could reduce the user effort and time required [3]. User interaction may include a rough selection of the initial ROI, which is subsequently utilized to segment the entire image. This type of segmentation may include manual interaction for correcting region boundaries to reduce segmentation errors [4].

Automatic algorithms would be able to produce reliable and repeatable segmentation results without the need for any user interaction. Over time, various automated conventional image segmentation algorithms have been developed, including thresholding as an intensity-based technique, edge-based [5] and region-based [2] methods, deformable models such as level set and active contour [6], clustering-based [7], and artificial neural network-based methods [8]. Thresholding and region-growing methods are two examples of region-based segmentation. Thresholding is the most basic approach to image segmentation. This algorithm directly divides the processing of the grayscale information of the image based on the gray value of distinct targets. The region-growing strategy is a typical region segmentation algorithm, and its fundamental idea is to consider similar properties of the pixels together to create a region. The approach needs to begin with the selection of a seed pixel and then surrounding similar pixels be combined into the region where the seed pixel is located. Edge detection is another conventional and basic approach in image segmentation that applies discontinuous local features of the image to detect the image edges.

In the clustering-based technique, the class term refers to the collection of similar elements. The feature space clustering method is utilized to segment the pixels within the image space into the corresponding feature space points. Human feature engineering, which is often used with machine learning approaches based on neural networks (NNs) or support vector machines (SVM), is another common segmentation method that is time-consuming due to the need for manual feature extraction [9]. There are also some challenging problems in medical image segmentation tasks, such as blurred and irregular borders, annotation bias, low contrast and imbalanced images, absence of texture contrast, sensitivity to contrast, imaging noise, etc. [10]. Nevertheless, incredible developments in medical image processing have occurred through NNs, and outstanding outcomes are consistent. Recently, motivated by the success of Deep Neural Networks (DNNs), researchers in the medical field have attempted to address a variety of issues using Deep Learning (DL) approaches, such as image denoising [11], image reconstruction [12], image registration [13], and also image segmentation [14]. These approaches have been effectively utilized for the semantic segmentation of natural images and have also found applications in the segmentation of medical images. Convolutional Neural Networks (CNNs) are key concepts in DL networks as feature extractors and highlight popular neural network architectures for this task. These architectures include the Fully Convolutional Network (FCN) [15], U-Net [16], Generative Adversarial Network (GAN) [17], Recurrent Neural Network (RNN) [18], and Auto-Encoder approaches [19]. This diverse range of DL architectures addresses various aspects of medical image segmentation, from handling volumetric data to capturing temporal relationships in

sequences, ultimately contributing to the advancement of precision medicine and diagnostic applications in the healthcare domain.

The complexity of targets motivates researchers to create a wide range of DL models in the field of medical image segmentation, which remains a significant challenge in this field and is one of the first issues that experts confront in diagnostic and treatment procedures. On the other hand, different properties, structures, and textures of the objects in the image affect the segmentation results. However, if the segmentation problem is investigated by concentrating on specific targets, the same approaches for each target could be found. In this case, we chose targets that drastically affect diagnosis and treatment procedures to provide a novel and informative target-based review of medical image segmentation, as shown in Figure 1. The "Vessel" is such a vital part of every organ that its accurate segmentation is critical for surgery and treatment planning, risk reduction in surgery, and clinical outcome evaluation. The "Tumor" almost has the potential to grow in every organ. So, accurate tumor segmentation leads to maximally safe resection and increases patient survival. Finally, "Pathology" underlies every field of medicine, from diagnosis, blood transfusion technology, and disease monitoring to cutting-edge genetic research.

It could be seen that the images within each group of targets exhibit visual similarities. These observations have prompted us to conduct a comprehensive systematic review of DL-based methods in medical image segmentation. The aim is to assist researchers in identifying the most suitable network for their specific target and addressing current challenges.

Figure 1. Visualization of three main groups of targets including tumor [20], vessel [21], and pathological images [22] for medical image segmentation.

The main contributions of our work are as follows:

(1) To employ the review protocol of the Preferred Reporting Items for Systematic Reviews and Meta-Analyses (PRISMA) search strategy to make the review accurate and reproducible.

(2) To provide a novel and informative target-based review on medical image segmentation, by summarizing the most popular networks applied for medical image segmentation and highlighting their advantages over other approaches.

(3) To select targets that have a drastic effect on diagnosis and treatment procedures, we review DNNs, datasets, and findings to provide an appropriate assessment in the medical image segmentation area.

The rest of the paper is organized as follows. Section 2 briefly introduces the main DNN models frequently used in medical image segmentation. Then, we describe the data description, pre-processing, and the most common performance metrics. Also, in the last part of section 2, we detail our review process. In section 3, we categorize the collected articles into three target-based groups: tumors, vessels, and pathological image segmentation. To clarify its most recent developments, each category was examined in detail for different body organs and imaging techniques. Finally, our conclusions are given in the last section.

2. Methodology

2.1. Deep learning (DL)

DL has been able to establish itself in medical image processing, especially image segmentation, since these tasks usually require high accuracy. CNNs as a class of artificial neural networks, provide the outcomes of convolving a certain number of filters with the input data and serving as feature extractors. In the following, we will mention some of the most commonly used neural network architectures for image segmentation tasks.

2.1.1. Fully Convolutional Network (FCN)

Long et al. [15] introduced the FCN, in which the final dense layer of CNN is replaced with a fully convolutional layer. In a study, Zhou et al. [23] employed the FCN comprising convolution and de-convolution section for the 2D semantic image segmentation of 19 different organs in 3D Computed Tomography (CT) scans.

2.1.2. U-Net

Ronneberger et al. [16] introduced U-Net, which has been extensively applied for medical image segmentation. The structure of U-Net is shown in Figure 2, which is established based on the delicate structure of FCN. Detecting or recognizing objects in medical images only based on the low-level features of the image is a very challenging issue. Moreover, obtaining accurate boundaries only from the semantic features of the image is impossible as there is no detailed image information. However, low-level and high-level features of the image in the U-Net are efficiently integrated through a combination of low-resolution and high-resolution feature maps using skip connections, which could be considered an ideal solution for fast and precise medical image segmentation.

Figure 2. U-Net architecture.

2.1.3. 3D U-Net

Due to the volumetric nature of most medical images, 3D convolution kernels are able to explore high-dimensional spatial correlation in the image. In this context, Icek et al. [24] extended the idea of U-Net to be applied to 3D data and introduced 3D U-Net, which processes 3D medical data. Milletari et al. [25] presented the V-Net, similar to the 3D U-Net structure. As demonstrated in Figure 3, residual connections could prevent vanishing gradients and improve network convergence. Therefore, it is arguable that designing deeper networks provides better feature

representation. Finally, it was applied to the V-Net using four down-sampling paths to design a deeper network. This architecture leads to higher performance in comparison with the 3D U-Net.

Figure 3. 3D U-Net architecture [25].

2.1.4. Generative Adversarial Network (GAN)

In 2014, Goodfellow et al. [17] presented an adversarial approach for learning a deep generative model as a GAN, which has been widely applied in several fields of computer vision. As depicted in Figure 4, it includes two parts: generative and adversarial networks. The generation network is the initial part that receives random noise and generates an image through this noise, and the second part, the adversarial network, combats against the network and makes a decision, whether the input image is “real” or “fake”. The first time, Luc et al. [26] applied the GAN for image segmentation that used the generative network for segmentation and trained the adversarial network as a classifier.

In medical image segmentation, the unbalanced pixels issue could not be resolved by the U-Net entirely, so Xue et al. [27] extended the architecture of U-Net to the generator of GAN and introduced a network named Segmentation Adversarial Network (SegAN), which led to better performance than the U-Net segmentation method.

Figure 4. GAN architecture.

2.1.5. Recurrent Neural Network (RNN)

RNN is invested in repeated connections and a particular type of loop architecture with a memory of prior knowledge, as shown in Figure 5. Long Short-Term Memory (LSTM) [18], one of the most popular RNNs, could maintain gradient flow by introducing a self-loop. In medical image segmentation, RNN is used to model the time dependency of image sequences while maintaining the total shape, smoothness, or regional homogeneity inside and outside the border. To model the temporal relationship between different brain magnetic resonance imaging (MRI) slices, Gao et al. [28] joined LSTM and CNN to enhance the accuracy of segmentation. FCN and RNN were combined by Bai et al. [29] to explore the spatiotemporal information for aortic sequence segmentation. By considering the context information relationship, local and global spatial features could be captured by RNN.

Recently, Xie et al. utilized a 2D structure of spatial Clockwork RNN (CW-RNN) in medical segmentation [30]. Context information extracted from the whole image could be encoded to represent each patch. It is extracted by splitting the entire image into a set of non-overlapping image patches. The proposed spatial CW-RNN model has semantic dependencies among them.

Figure 5. RNN architecture.

2.1.6. Auto-Encoder based DL Architectures

To compress the input into a latent-space representation, an Auto-Encoder (AE), including the neural network encoder, is used with values similar to inputs intended in the back-propagation algorithm. This network includes a decoder that restores the latent representation input and an encoder that compresses the input to a latent representation (Figure 6).

Zimmerer et al. [19] presented a segmentation method based on context-encoding and variational AE for brain T2-weighted images. They attempted to discover anomalies at the pixel level by using model-internal latent representation deviations and reconstructing a more expressive error. Vaidhya et al. [31] used unsupervised 3D stacked denoising auto-encoders to detect and segment glioma patches in brain MR images. Baur et al. [32] combined both concepts of GANs and AEs arguing that AEs suffer from memorization and tend to produce blurry images, and GANs have been shown to produce very sharp images due to adversarial training. They leveraged a deep generative model in the form of spatial variational AEs to build a new model for anomaly segmentation in brain MR images.

Figure 6. AE-based DL architecture.

2.2. Data Description

Since DNNs gather information from tens of thousands of images, their performance depends on using large datasets. In many computer vision tasks, preparing a large dataset is simple, but collecting and labeling representative, high-quality datasets in medical applications is challenging. This is due to the variety of data acquisition sources and the time it takes to label with a specialist physician's annotation as a ground truth. However, a wide range of public databases for various medical applications have been

collected and annotated in recent years. This would provide the possibility of using DL models on a wide range of targets and also allow the comparison of studies' results. Here is a summary of the most widely used public databases available for medical image segmentation applications based on our targets:

2.2.1. Tumor Segmentation

- Brain Tumor Segmentation

Brain Tumor Segmentation (BraTS) database is a well-accepted benchmark for brain tumor segmentation studies using DL. This database is published annually and includes MRI scans of patients with high-grade and low-grade glioma in four MRI sequences (T1, T2, T1-Gd, and FLAIR), and has ground truth for each glioma sub-regions [33].

- Liver Tumor Segmentation

Due to the importance of automatic liver tumor segmentation, in a challenge in 2017, liver tumor segmentation (LiTS17) data was released. The training dataset contains 130 CT scans, whereas the test dataset contains 70 CT scans, which are segmented by various clinical sites around the world. The LiTS image data and manual annotations will be made publicly available through an online evaluation system as a benchmarking resource. LiTS has been used frequently in automatic liver tumor segmentation studies. It is noteworthy that first, most studies for accurate liver tumor segmentation focused on liver tissue segmentation [34]. 3D Image Reconstruction for Comparison of Algorithm Database (3D-IRCADb) is a database that contains 3D CT scans of ten women and ten men with liver cancers, along with specialist ground truth manual segmentation of different objects of interest [35].

- Lung Tumor Segmentation

In [36], a radiogenomic dataset containing images of Non-Small Cell Lung Cancer (NSCLC) patients has been provided. It contains CT images, Positron Emission Tomography (PET)/CT images, and specialist annotations of the tumors as ground truth.

2.2.2. Blood Vessel Segmentation

For the segmentation of blood vessels in the head and neck, brain, retina, abdomen, and coronary arteries utilizing imaging techniques such as MRI, OCT, ophthalmoscopy, CTA, and X-Ray, various databases have been released, which are further referenced. Also, in the literature, the available datasets of DRIVE [37], TOPCON [38], STARE [39], CHASE_DB1 [40], RITE [41], HRF [42], RC-SLO [43], IOSTAR [44], and IndoCyanine Green (ICG) angiography [45] for retinal organ and IRCAD [35] and MSD [46] related to liver vessel segmentation have been used. Also, a review has been done on the organs of the brain, abdomen, coronary, and head and neck, whose datasets are not publicly available.

2.2.3. Pathological Image Segmentation

Among the datasets introduced in this field, CAMELYON16, CAMELYON17 [47], the KMC dataset (also known as the Kumar dataset) [48], and the Pathological Myopia (PALM) dataset [49] stand out as prominent sources of pathological image data, each offering unique insights and challenges for research in this domain.

2.3. Data Preprocessing

Before feeding raw image data to the network, some standard pre-processing techniques are applied to the multi-modal medical images, such as noise removal operations, image registration, skull-stripping, intensity bias correction, and normalization. This step is crucial in medical image segmentation because raw data has various brightness and contrast. They contain irrelevant structures and noise that are relevant to different imaging protocols and acquisition devices [50].

Data preprocessing involves essential steps to prepare the data for further analysis. Noise removal is the process of eliminating unwanted variations or irrelevant information that could distort results. Noise removal is crucial to eliminate artifacts or unwanted variations in medical images, such as MRI scans or X-rays, ensuring that the segmentation algorithms can accurately delineate structures of interest like tumors or organs. Enhancement techniques improve data quality by enhancing features and patterns, enhancing clarity, or adjusting contrast [51]. Enhancement techniques are employed to improve the visibility of subtle features or boundaries within medical images, aiding in the precise identification and segmentation of anatomical structures. These preprocessing steps collectively ensure that the data used in research is of high quality, representative, and suitable for accurate analysis or modeling, enhancing the reliability and robustness of the results obtained.

Moreover, collecting large amounts of data and annotating them by a specialist in medical image analysis is time-consuming and costly. On the other hand, low bias and high variance cause overfitting in training data. Image data augmentation is one of the most widely used solutions to this problem [50]. This method helps us improve the dataset's size and quality in the training phase to build a more powerful DL model by applying a set of transformations in the data or feature space [52]. Image data augmentation methods generally fall into two categories: creating new data by making specific changes to existing images using basic image manipulations such as geometric and color space transformations, mixing images, random erasing, and kernel filters. Creating synthetic data using crowdsourcing and DL-based techniques, including adversarial training, neural style transfer, and GAN data augmentation [53]. Image data augmentation is also helpful in creating faster convergence and improving model generalization. In this context, these preprocessing techniques not only enhance the accuracy and reliability of medical image segmentation but also contribute significantly to clinical diagnosis and treatment planning.

2.4. Performance Metrics

The efficacy of the image segmentation algorithms is evaluated regard to the ground truth, which is provided by experts. For quantitative studies of different segmentation methods and the possibility of comparing their performance, typical uniform and standard evaluation metrics are utilized. However, numerous definitions for a specific metric and applications of an algorithm for different object/organ/structure segmentation would cause challenges in introducing standard evaluation criteria.

Various categories are recommended for evaluation metrics of medical image segmentation, including spatial overlap-based, spatial distance-based, volume-based, probabilistic, and information theoretical-based metrics [54]. Based on our approach, we introduced the most common metrics that fall into the first category. As shown in Figure 7, all spatial overlap-based metrics could be obtained from four basic error rate definitions: true positive (*TP*), false positive (*FP*), true negative (*TN*), and false negative (*FN*). In the following, some criteria are introduced that have been used in most studies.

Figure 7. Schematic illustration of four basic error rate definitions.

- Dice Similarity Coefficient

The Dice Similarity Coefficient (*DSC*) is used to evaluate the similarity between the two sets. This criterion is the overlap between the segmentation results and ground truth annotation. It is widely used to evaluate segmentation methods and takes a value between 0 and 1. The closer this criterion is to 1, the greater the similarity between the segmentation masks. *DSC* is expressed as Equation 1.

$$DSC = 2\frac{\left|S_{Ground\,Truth} \cap S_{Segmentation\,Results}\right|}{\left|S_{Ground\,Truth}\right| + \left|S_{Segmentation\,Results}\right|} = \frac{2TP}{2TP + FP + FN} \tag{1}$$

- True Positive Rate

The True Positive Rate (*TPR*), called Recall or Sensitivity, calculates the percentage of actual positive pixels/voxels in ground truth, which are correctly segmented by the algorithm. It is calculated as Equation 2.

$$TPR = \frac{TP}{TP + FN} \tag{2}$$

- True Negative Rate

The True Negative Rate (*TNR*), also called Specificity, calculates the percentage of actual negative pixels/voxels in the ground truth, which are correctly segmented (as background) by the algorithm. This could be stated as Equation 3.

$$TNR = \frac{TN}{TN + FP} \tag{3}$$

- Accuracy

Accuracy (*Acc*) is the ability of the system to distinguish between foreground and background in the image that measures the true positive and true negative voxels/pixels in all predictions. This could be stated as Equation 4.

$$Acc = \frac{TN + TP}{TN + TP + FP + FN} \tag{4}$$

2.5. Review Process

Since the primary concern in the treatment protocol is the target, this study provided a quick configuration of state-of-the-art DL models for medical image segmentation based on specific targets: tumor, vessel, and pathology. This new classification of articles could affect accurate access to practical

articles in the clinic from now on. In this paper, we attempted to provide a simple-to-use and presentative framework that focused on target-based medical image segmentation methods based on DL techniques.

2.5.1. Study selection

We employed the review protocol of the PRISMA search strategy to make the review accurate and reproducible (www.prisma-statement.org) [55]. This search strategy consists of 4 steps: identification, screening, eligibility, and included. The following are the details of the PRISMA statement:

Identification stage: The results were obtained using the following research terms: (medical image segmentation*) AND (deep learning*). These keywords have been searched to obtain the latest literature from the Google Scholar search engine and the PubMed database, and the results are represented in Figure 8, queried on April 30, 2023.

Screening stage: According to an exponential growth in the number of published articles between 2015 and 2023, this limitation was considered. As a result, we obtained 789,581 records, of which 775,905 records were eliminated based on duplication and the considered year limitation. Also, due to the vast number of articles on brain tumors, articles only related to the last two years were considered. The titles and abstracts of the remaining articles have been reviewed and 13,247 records were eliminated due to the consideration of specific targets for review.

Eligibility stage: Due to reasons such as the unavailability of full-text articles, the evaluation criteria considered in this review, and the use of similar methods in some articles, 311 records have been deleted.

Included stage: Finally, 118 articles were included in the systematic review. Of these articles, 34%, 13%, 8%, 28%, and 17% records are related to the brain tumor, liver, lung, blood vessel, and pathology segmentation, respectively. According to the PRISMA statement, details about the exclusion and inclusion of papers are shown in Figure 9.

2.5.2. Extracted Data

In order to better summarize the various methods for each target, a table is provided that contains the organ/modality that shows the organ and imaging techniques that are used, the DL network architecture and its approach, evaluation metrics, and finally, the dataset which is applied for evaluating the proposed algorithm. The tables compare and summarize related methods and identify the challenges for successful methods of DL for medical image segmentation tasks. This study has aimed to investigate the application of DL technology in medical image segmentation over the past seven years. The strengths and limitations of network structure and methods are also being investigated.

Figure 8. The number of publications for target-based segmentation (till April 2023).

Figure 9. Inclusion and exclusion criteria for selection of articles for systematic review according to the PRISMA guidance.

3. Results

3.1. Tumor Segmentation

Tumor segmentation represents the correct identification of the spatial location of a tumor. Therefore, reliable and accurate tumor segmentation is essential for accurate diagnosis and treatment planning,

especially in vital organs of the human body, such as the lung, liver, and brain [56]. In the following, tumor segmentation is investigated for three vital targets: The lung, liver, and brain.

3.1.1. Brain Tumor Segmentation

Brain tumor segmentation is associated with some issues due to the blurred and irregular boundaries of the tumor and the variety of its location and forms [57, 58]. Furthermore, because the brain tumor segmentation poses challenges such as annotation bias, low contrast, and imbalanced images, researchers are constantly looking for novel strategies to improve their results.

Among all types of brain tumors, glioma is the most common and invasive type of brain tumor with high and low grades, which highly determines the patient survival rate. Therefore, accurate segmentation and grading of gliomas are essential in diagnosis and treatment planning [59]. Recently, some DL-based brain tumor segmentation studies have achieved good results by including the classification of glioma grades in their approach. For example, Yogananda et al. [60] simplified the complex segmentation problem by first classifying the high-grade glioma (HGG) and low-grade glioma (LGG) cases with a simple CNN classifier and then performing their segmentation approaches. Also, brain tumor images could be analyzed in 2D slices or 3D volumes, leading to some studies that trained the network directly using 3D volumes [61, 62], or images were fed slice to slice to the network [63, 64]. For example, Kaldera et al. [65] used 2D slices only in the axial view, assuming that a higher resolution of the tumor could be seen in this view. Tripathi et al. incorporate internal residual connections in the encoder and decoder to transfer feature maps to preserve boundary and pixel details [66].

One of the practical challenges in brain tumor segmentation is the image imbalance between healthy tissue and tumoral tissue [67]. In [68], a proposed 3D CNN as a helpful solution addressed the data imbalance issue (image imbalance between foreground and background). Given that a large part of the images is healthy texture or background, by adding a practical loss function, a new hybrid model (IOUC-3DSFCNN) is proposed that has better performance to solve this problem.

DL-based brain tumor segmentation methods in the following four general categories, including CNNs, RNNs, AEs, and GANs, have been used frequently in recent studies. Many studies with various innovations have been performed to segment brain tumors using CNNs [69, 70]. In comparison, RNN, which could represent time series inputs, has been used less than CNN in brain tumor segmentation tasks [71, 72]. Recently, GANs and AEs have been utilized for brain tumor segmentation [73, 74]. Different architectures and training details could affect the networks' performance. The use of assembling the model is a recommended approach that results in an unbiased and robust brain tumor segmentation outcome by averaging the variance of the models [62, 75]. Despite the high efficiency of DL-based brain tumor segmentation models, the results of these methods require expert correction and interventions.

Therefore, interactive methods that allow physician intervention in the segmentation results have been considered recently [76, 77]. In recent years, the number of studies conducted on the segmentation of brain tumors based on DL has grown rapidly; therefore, some recent studies have been reviewed (Table 1).

3.1.2. Liver Tumor Segmentation

In recent years, liver cancer has surpassed lung cancer as the fourth leading cause of death worldwide [78]. The liver could be affected by various tumors with different visual appearances. Secondary tumors, including lung, breast, colon, etc., metastasize to the liver in addition to tumors that originate in the liver,

like hepatocellular carcinoma. Due to their heterogeneous and diffusive shape, automatic segmentation of liver tumors is a challenging task. Between 2017 and 2019, several public challenges and competitions centered around liver and liver tumor segmentation were organized. These challenges, including Sliver07 and 3D Segmentation in the Clinic: A Grand Challenge [79], primarily featured conventional methods like level set techniques, thresholding, and machine learning approaches. However, it became evident that these traditional methods struggled to match the performance of deep learning techniques. While significant progress has been made in achieving near-human precision in liver segmentation, robustly segmenting liver tumors remains a formidable obstacle. This challenge is exacerbated by the lack of publicly datasets containing labels for both liver and liver tumors. Access to private datasets is limited due to privacy concerns and the labor-intensive process of image annotation. The CHAOS challenge [80] was launched in 2019 to evaluate the effectiveness of multi-modal systems that leveraged voxel information for liver segmentation across both CT and MRI volumetric images.

Table 2 summarizes recent studies, including various DL models for liver tumor segmentation, which have acceptable results.

3.1.3. Lung Tumor Segmentation

Lung cancer is one of the most deadly kinds of cancer [81]. Hence, image segmentation would be a critical process in detecting and characterizing lung tumors [82]. Due to the limitations and complexity of diagnosing and classifying lung tumors with manual segmentation methods, automated segmentation methods with acceptable outcomes have been presented for accurate lung tumor segmentation [81]. These automated methods not only improve the precision of lung tumor segmentation but also offer the potential for more efficient and consistent diagnoses, ultimately playing a pivotal role in improving patient outcomes and the overall management of lung cancer.

The great success of DL methods for analyzing lung tumors has significantly improved the segmentation, classification, and identification tasks. Table 3 provides a summary of recent studies, including various DL models for lung tumor segmentation. In these studies, imaging modalities such as PET-CT, 2D and 3D CT, and bronchoscopy have been used to show non-small-cell lung cancer, lung nodules, tumors of soft tissue sarcoma, benign and malignant, and lung cancer.

Clinically, maximum tumor removal without damage to surrounding healthy tissues (organs at risk) is an essential goal in neuro-oncology. Automatic segmentation with deep learning methods has recently received much attention in tumor segmentation. Deep convolutional networks, especially U-Net, have received the most attention for this task; however, in some studies, the use of GAN networks has been recommended. The main challenge in using these structures is the large number of model parameters and the need for a large amount of data for network training and acceptable generalization. This problem has been solved recently using more compact networks, such as capsule networks with fewer parameters.

Table 1. Summary of DL approaches in brain tumor segmentation.

3.2. Blood Vessel Segmentation

Blood vessel segmentation is a topic of high interest in medical image processing since vessel analysis is crucial for the execution and treatment planning, diagnosis, and evaluation of clinical outcomes in

different fields, such as neurosurgery, ophthalmology, oncology, and laryngology. Semi-automatic or automatic vessel segmentation would greatly assist clinicians in this regard. A variety of medical imaging modalities are being employed in clinical practice, and selecting an appropriate segmentation method is mandatory to deal with the characteristics of adopted imaging technique (e.g., vessel contrast, noise, and resolution) [97].

The process of manually segmenting blood vessels is both time-consuming and lacks consistency and reproducibility between different operators. In contrast, semi-automatic or fully automatic vessel segmentation methods necessitate the involvement of at least one expert clinician to either perform the segmentation or assess the obtained segmentation results. Moreover, the development and evaluation of these algorithms suffer from lack of support since publicly image datasets that include Ground Truth are now limited to specific anatomical regions, such the retina. Nonetheless, the utilization of automatic or semi-automatic blood vessel segmentation methods could provide assistance to clinicians. As a result, these areas hold significant importance in medical research, as evidenced by the substantial annual publication rate in this domain [97]. In recent years, the popularity of DL approaches in medical imaging has grown because of their robust capability in extracting features, precise classification, and adaptability [98]. Nonetheless, given the rapid advancements in the field, there is a need for updated reviews to assess and summarize the current state of the art.

Table 4 provides a summary of recent studies, including various DL models for vessel segmentation. In these studies, imaging modalities such as the MRI, ophthalmoscope, optical coherence tomography (OCT), CT, and CT angiography (CTA) have been used to show the vessels of organs such as the brain, retina, esophageal, abdominal, coronary, type B aortic dissection (TBAD), liver, and head and neck. According to Table 4, deep learning networks have been widely used in blood vessel segmentation. The researchers used CNN and U-Net networks more because of their good performance on the databases. In addition, many authors have proposed various improved models such as the U-Net CNN, the DV-Net, TransFusionNet, the R2U-Net, the scale-space approximated CNN, the Hard Attention Net, ResDO-UNet, etc. for blood vessel segmentation. Also, due to the importance of retinal vessels, most studies on this organ have been done using the ophthalmoscope imaging modality. The most common performance evaluation metrics have been the proposed methods for blood vessel segmentation, *ACC* and *TPR*, which on average in this survey are 0.94±0.05 and 0.83±0.08, respectively.

Table 2. Summary of DL approaches in liver tumor segmentation

3.3. Pathology Image Segmentation

The digitized pathology slides provide opportunities for clinical diagnosis that could assist pathologists and researchers in disease monitoring. Because of the success of DL, digital pathology is rapidly progressing. Prior to DL's popularity in the analysis of medical images, pathology images were difficult to analyze due to their complexity [118]. However, digital pathology image segmentation using DL could not be accomplished in interpreting whole slide images to detect tumor regions [119] and lymph node metastases [47].

In 2012, a grand challenge in histopathology was held and focused only on mitosis detection in breast cancer histological images [120]. This was the first time in a histopathology challenge where DL methods outperformed other methods based on handcrafted features and smoothed the way for future use of CNNs. For the first time in 2013, pathology image segmentation made its way through the rapid progress of DL by using deep max-pooling CNNs to detect mitosis in breast histology images [121].

Most efforts to date have focused on developing neural network architectures to enhance the performance of different computational pathological tasks. U-Net has been commonly used in several applications [122]. It has been implemented in an end-to-end architecture and to overcome the challenge of limited medical databases, it has extensively used data augmentation to better leverage the available annotation examples [123].

Medical image segmentation has exponentially grown in the last few years. However, unfortunately, the pathological images are left out of this rapidly growing storm due to the challenges it faces in this area. Access to large well-annotated datasets, context switching between workflows, and lack of health economics are some key challenges that slow down DL and make pathologists hesitant to adopt it [123].

In Table 5, we only consider recent studies that have yielded acceptable results in this field. As shown in Table 5, convolutional networks have received much attention from researchers in pathology image segmentation. In the meantime, by introducing U-Net in pathology image segmentation, the accuracy of segmentation has increased.

Table 3. Summary of DL approaches in lung tumor segmentation.
Table 4. Summary of DL approaches in blood vessel segmentation.
Table 5. Summary of DL approaches in pathology image segmentation.

4. Conclusion

- Nowadays, due to the penetration of DL in medical image segmentation, many articles have been published in this field and researchers have been able to segment almost all types of medical images. Considering the complexity and variation of different targets, DL models have been proposed that specify each target in medical image segmentation. There are many available targets to review in this field, such as vessel, tumor, pathology, cardiac, skin cancer, lesion, and bone segmentation, and each one has considerable importance. This paper first summarized the most popular networks applied for medical image segmentation and highlighted their different advantages. To provide a novel and informative target-based review on medical image segmentation, we decided to select targets that drastically affect diagnosis and treatment procedures, as shown in Figure 1. "Vessel" is a vital part of every organ that accurate segmentation of it is a crucial issue for surgery and treatment planning, minimization of the risks of surgery, and evaluation of clinical outcomes. "Tumor" almost has the potential to grow in every organ and accurate segmentation of different tumors leads to maximally safe resection of them and increases patient survival. Finally, "pathology" underlies every field of medicine, from diagnosis, blood transfusion technology, and disease monitoring to cutting-edge genetic research. In reviewing the mentioned targets, this issue is highly realizable, in that a variety of networks are provided for each target, and the most notable results for each target occur with a specific network. In this case, for brain and liver tumors and vessel images, different kinds of residual networks, GAN and CNN, respectively, and for lung tumors and pathology images, different types of U-Net had the best results. Along with targets, we reviewed DNNs, datasets, and results to provide an appropriate assessment in this area. Although enormous dataset challenges are a deniable fact, all indications point to the significant role of DL techniques in medical image segmentation.

- **Open problems and challenges:** Although deep learning has shown significant results in medical image segmentation, it has yet to be placed in a suitable place in the clinical routine. This cross-disciplinary field deals with complex pathological medical data on the one hand, and on the other hand

with the field of engineering, where the adaptation of these two fields has yet to happen well. In fact, many parts of medical knowledge that are effective in making final decisions could not be understood by artificial intelligence and vice versa. Fortunately, the rapid growth of deep learning methods has been realized, and today, more interpretable approaches such as explainable artificial intelligence have emerged, which have provided the expert with high interaction and confidence in artificial intelligence methods.

- **Future directions:** With the increasing implementation of deep learning models in critical medical applications, the need for transparency and interpretability becomes paramount. Integrating an examination of explainable AI (XAI) techniques within this systematic review can help us realize how these methods are shaping the landscape of medical image segmentation. Understanding and expressing how and why deep learning models arrive at specific segmentation decisions is essential for gaining the trust of healthcare professionals and ensuring safe and effective clinical implementation. Furthermore, XAI plays a pivotal role in addressing ethical concerns, ensuring accountability, and meeting regulatory requirements in the healthcare sector. Thus, exploring the current state and future potential of XAI within medical image segmentation could be a pivotal component of future systematic reviews in this field, offering insights that are not only academically significant but also practically indispensable for the advancement of AI in healthcare.

Acknowledgment

The authors declare that they have no conflict of interest.

References

1. Liu, T., Liu, J., Ma, Y., et al., "Spatial feature fusion convolutional network for liver and liver tumor segmentation from CT images", Medical Physics, **48**(1), pp. 264-272 (2021). DOI: 10.1002/mp.14585.
2. Shrivastava, N., and Bharti, J., "Automatic Seeded Region Growing Image Segmentation for Medical Image Segmentation: A Brief Review", International Journal of Image and Graphics, **20**(03), pp. 2050018 (2020). DOI: 10.1142/S0219467820500187.
3. Krissian, K., Carreira, J.M., Esclarin, J., and Maynar, M., "Semi-automatic segmentation and detection of aorta dissection wall in MDCT angiography", Medical image analysis, **18**(1), pp. 83-102 (2014). DOI: 10.1016/j.media.2013.09.004.
4. Haque, I.R.I., and Neubert, J., "Deep learning approaches to biomedical image segmentation", Informatics in Medicine Unlocked, **18**, pp. 100297 (2020). DOI: 10.1016/j.imu.2020.100297.
5. Salman, N., Ghafour, B., and Hadi, G., "Medical Image Segmentation Based on Edge Detection Techniques", Advances in Image and Video Processing, **3** (2015). DOI: 10.14738/aivp.32.1006.
6. Kazerooni, A.F., Ahmadian, A., Serej, N.D., et al., "Segmentation of brain tumors in MRI images using multi-scale gradient vector flow", 2011 Annual International Conference of the IEEE Engineering in Medicine and Biology Society, IEEE, pp. 7973-7976 (2011). DOI: 10.1109/IEMBS.2011.6091966.
7. Rizi, F.Y., Bidgoli, J.H., Ahmadian, A., and Alirezaie, J., "An Efficient Fuzzy Connectivity Method for Airway Tree Segmentation Using Fuzzy C-mean Algorithm", 4th Kuala Lumpur International Conference on Biomedical Engineering 2008, Springer Berlin Heidelberg, Berlin, Heidelberg, pp. 501-505 (2008). DOI: 10.22038/IJMP.2009.7392.
8. Işın, A., Direkoğlu, C., and Şah, M., "Review of MRI-based brain tumor image segmentation using deep learning methods", Procedia Computer Science, **102**, pp. 317-324 (2016). DOI: 10.22038/IJMP.2009.7392.

9. Yuheng, S., and Hao, Y., "Image segmentation algorithms overview", arXiv preprint arXiv:1707.02051, (2017). DOI: 10.48550/arXiv.1707.02051.
10. Bi, W.L., Hosny, A., Schabath, M.B., et al., "Artificial intelligence in cancer imaging: Clinical challenges and applications", CA Cancer J Clin, **69**(2), pp. 127-157 (2019). DOI: 10.3322/caac.21552.
11. Tian, C., Fei, L., Zheng, W., et al., "Deep learning on image denoising: An overview", Neural Networks, 131, pp. 251-275 (2020). DOI: 10.1016/j.neunet.2020.07.025.
12. Farnia, P., Mohammadi, M., Najafzadeh, E., et al., "High-quality photoacoustic image reconstruction based on deep convolutional neural network: towards intra-operative photoacoustic imaging", Biomed Phys Eng Express, **6**(4), pp. 045019 (2020). DOI: 10.1088/2057-1976/ab9a10.
13. Haskins, G., Kruger, U., and Yan, P., "Deep learning in medical image registration: a survey", Machine Vision and Applications, **31**, pp. 1-18 (2020). DOI: 10.48550/arXiv.1903.02026.
14. Mahmoudi, T., Kouzahkanan, Z.M., Radmard, A.R., et al., "Segmentation of Pancreatic Ductal Adenocarcinoma (PDAC) and surrounding vessels in CT images using deep convolutional neural networks and texture descriptors", bioRxiv, pp. 2021.06.09.447508 (2021). DOI: 10.1101/2021.06.09.447508.
15. Long, J., Shelhamer, E., and Darrell, T., "Fully convolutional networks for semantic segmentation", Proceedings of the IEEE conference on computer vision and pattern recognition, pp. 3431-3440 (2015). DOI: 10.48550/arXiv.1411.4038.
16. Ronneberger, O., Fischer, P., and Brox, T., "U-net: Convolutional networks for biomedical image segmentation", International Conference on Medical image computing and computer-assisted intervention, Springer, pp. 234-241 (2015). DOI: 10.1007/978-3-319-24574-4_28.
17. Goodfellow, I.J., Pouget-Abadie, J., Mirza, M., et al., "Generative adversarial networks", arXiv preprint arXiv:1406.2661, (2014). DOI: 10.48550/arXiv.1406.2661.
18. Hochreiter, S., and Schmidhuber, J., "Long short-term memory", Neural computation, **9**(8), pp. 1735-1780 (1997). DOI: 10.1162/neco.1997.9.8.1735.
19. Zimmerer, D., Kohl, S.A., Petersen, J., et al., "Context-encoding variational autoencoder for unsupervised anomaly detection", arXiv preprint arXiv:1812.05941, (2018). DOI: 10.48550/arXiv.1812.05941.
20. Valente, I.R.S., Cortez, P.C., Neto, E.C., et al., "Automatic 3D pulmonary nodule detection in CT images: a survey", Computer methods and programs in biomedicine, **124**, pp. 91-107 (2016). DOI: 10.1016/j.cmpb.2015.10.006.
21. Ma, Y., Li, X., Duan, X., et al., "Retinal Vessel Segmentation by Deep Residual Learning with Wide Activation", Computational Intelligence and Neuroscience, **2020**, pp. 8822407 (2020). DOI: 10.1155/2020/8822407.
22. Menter, T., Nicolet, S., Baumhoer, D., et al., "Intraoperative frozen section consultation by remote whole-slide imaging analysis–validation and comparison to robotic remote microscopy", Journal of clinical pathology, **73**(6), pp. 350-352 (2020). DOI: 10.1136/jclinpath-2019-206261.
23. Zhou, X., Ito, T., Takayama, R., et al., *Three-dimensional CT image segmentation by combining 2D fully convolutional network with 3D majority voting*, in *Deep Learning and Data Labeling for Medical Applications*. 2016, Springer. p. 111-120. DOI: 10.1007/978-3-319-46976-8_12.
24. Çiçek, Ö., Abdulkadir, A., Lienkamp, S.S., et al., "3D U-Net: learning dense volumetric segmentation from sparse annotation", International conference on medical image computing and computer-assisted intervention, Springer, pp. 424-432 (2016). DOI: 10.48550/arXiv.1606.06650.
25. Milletari, F., Navab, N., and Ahmadi, S.-A., "V-net: Fully convolutional neural networks for volumetric medical image segmentation", 2016 fourth international conference on 3D vision (3DV), IEEE, pp. 565-571 (2016). DOI: 10.48550/arXiv.1606.04797.
26. Luc, P., Couprie, C., Chintala, S., and Verbeek, J., "Semantic segmentation using adversarial networks", arXiv preprint arXiv:1611.08408, (2016). DOI: 10.48550/arXiv.1611.08408.
27. Xue, Y., Xu, T., Zhang, H., et al., "Segan: Adversarial network with multi-scale l 1 loss for medical image segmentation", Neuroinformatics, **16**(3), pp. 383-392 (2018). DOI: 10.48550/arXiv.1706.01805.
28. Gao, Y., Phillips, J.M., Zheng, Y., et al., "Fully convolutional structured LSTM networks for joint 4D medical image segmentation", 2018 IEEE 15th International Symposium on Biomedical Imaging (ISBI 2018), IEEE, pp. 1104-1108 (2018). DOI: 10.1109/ISBI.2018.8363764.
29. Bai, W., Suzuki, H., Qin, C., et al., "Recurrent neural networks for aortic image sequence segmentation with sparse annotations", International Conference on Medical Image Computing and Computer-Assisted Intervention, Springer, pp. 586-594 (2018). DOI: 10.48550/arXiv.1808.00273.
30. Xie, Y., Zhang, Z., Sapkota, M., and Yang, L., "Spatial clockwork recurrent neural network for muscle perimysium segmentation", International Conference on Medical Image Computing and Computer-Assisted Intervention, Springer, pp. 185-193 (2016). DOI: 10.1007/978-3-319-46723-8_22.
31. Vaidhya, K., Thirunavukkarasu, S., Alex, V., and Krishnamurthi, G., "Multi-modal brain tumor segmentation using stacked denoising autoencoders", BrainLes 2015, Springer, pp. 181-194 (2015). DOI: 10.1007/978-3-319-30858-6_16.

32. Baur, C., Wiestler, B., Albarqouni, S., and Navab, N., "Deep autoencoding models for unsupervised anomaly segmentation in brain MR images", International MICCAI Brainlesion Workshop, Springer, pp. 161-169 (2018). DOI: 10.1007/978-3-030-11723-8_16.
33. Menze, B.H., Jakab, A., Bauer, S., et al., "The multimodal brain tumor image segmentation benchmark (BRATS)", IEEE transactions on medical imaging, **34**(10), pp. 1993-2024 (2014). DOI: 10.1109/TMI.2014.2377694.
34. Bilic, P., Christ, P.F., Vorontsov, E., et al., "The liver tumor segmentation benchmark (lits)", arXiv preprint arXiv:1901.04056, (2019). DOI: 10.1016/j.media.2022.102680.
35. Soler, L., Hostettler, A., Agnus, V., et al., "3D image reconstruction for comparison of algorithm database", IRCAD, Strasbourg, France, Tech. Rep (2010). DOI: 10.1109/CRC.2018.00010.
36. Bakr, S., Gevaert, O., Echegaray, S., et al., "A radiogenomic dataset of non-small cell lung cancer", Scientific data, **5**, pp. 180202-180202 (2018). DOI: 10.1038/sdata.2018.202.
37. Staal, J., Abràmoff, M.D., Niemeijer, M., et al., "Ridge-based vessel segmentation in color images of the retina", IEEE transactions on medical imaging, **23**(4), pp. 501-509 (2004). DOI: 10.1109/TMI.2004.825627.
38. Cheng, J., Tao, D., Quan, Y., et al., "Speckle reduction in 3D optical coherence tomography of retina by A-scan reconstruction", IEEE transactions on medical imaging, **35**(10), pp. 2270-2279 (2016). DOI: 10.1109/TMI.2016.2556080.
39. Hoover, A.D., Kouznetsova, V., and Goldbaum, M., "Locating blood vessels in retinal images by piecewise threshold probing of a matched filter response", IEEE Transactions on Medical imaging, **19**(3), pp. 203-210 (2000). DOI: 10.1109/42.845178.
40. Fraz, M.M., Remagnino, P., Hoppe, A., et al., "An ensemble classification-based approach applied to retinal blood vessel segmentation", IEEE Transactions on Biomedical Engineering, **59**(9), pp. 2538-2548 (2012). DOI: 10.1109/TBME.2012.2205687.
41. Hu, Q., Abràmoff, M.D., and Garvin, M.K., "Automated separation of binary overlapping trees in low-contrast color retinal images", Springer, pp. 436-443. DOI: 10.1007/978-3-642-40763-5_54.
42. Budai, A., Bock, R., Maier, A., et al., "Robust Vessel Segmentation in Fundus Images", International Journal of Biomedical Imaging, **2013**, pp. 154860 (2013). DOI: 10.1155/2013/154860.
43. Zhang, J., Dashtbozorg, B., Bekkers, E., et al., "Robust retinal vessel segmentation via locally adaptive derivative frames in orientation scores", IEEE transactions on medical imaging, **35**(12), pp. 2631-2644 (2016). DOI: 10.1109/TMI.2016.2587062.
44. Abbasi-Sureshjani, S., Smit-Ockeloen, I., Zhang, J., and Romeny, B.T.H., "Biologically-inspired supervised vasculature segmentation in SLO retinal fundus images", Springer, pp. 325-334. DOI: 10.1007/978-3-319-20801-5_35.
45. Ciulla, T.A., Harris, A., and Martin, B.J., "Ocular perfusion and age-related macular degeneration", Acta Ophthalmologica Scandinavica, **79**(2), pp. 108-115 (2001). DOI: 10.1034/j.1600-0420.2001.079002108.x.
46. Simpson, A.L., Antonelli, M., Bakas, S., et al., "A large annotated medical image dataset for the development and evaluation of segmentation algorithms", arXiv preprint arXiv:1902.09063, (2019). DOI: 10.48550/arXiv.1902.09063.
47. Bejnordi, B.E., Veta, M., Van Diest, P.J., et al., "Diagnostic assessment of deep learning algorithms for detection of lymph node metastases in women with breast cancer", Jama, **318**(22), pp. 2199-2210 (2017). DOI: 10.1001/jama.2017.14585.
48. Kumar, N., Verma, R., Anand, D., et al., "A multi-organ nucleus segmentation challenge", IEEE transactions on medical imaging, **39**(5), pp. 1380-1391 (2019). DOI: 10.1109/TMI.2019.2947628.
49. Fu, H., Li, F., Orlando, J.I., et al., "Palm: Pathologic myopia challenge", IEEE Dataport, (2019). DOI:10.21227/55pk-8z03.
50. Zhou, T., Ruan, S., and Canu, S., *A review: Deep learning for medical image segmentation using multi-modality fusion*. 2020. DOI: 10.1016/j.array.2019.100004.
51. Batini, C., Cappiello, C., Francalanci, C., and Maurino, A., "Methodologies for data quality assessment and improvement", ACM computing surveys (CSUR), **41**(3), pp. 1-52 (2009). DOI: 10.1145/1541880.1541883.
52. Nalepa, J., Marcinkiewicz, M., and Kawulok, M., "Data Augmentation for Brain-Tumor Segmentation: A Review", Frontiers in Computational Neuroscience, **13**(83) (2019). DOI: 10.3389/fncom.2019.00083.
53. Shorten, C., and Khoshgoftaar, T., "A survey on Image Data Augmentation for Deep Learning", Journal of Big Data, **6** (2019). DOI: 10.1186/s40537-019-0197-0.
54. Taha, A.A., and Hanbury, A., "Metrics for evaluating 3D medical image segmentation: analysis, selection, and tool", BMC Medical Imaging, **15**(1), pp. 29 (2015). DOI: 10.1186/s12880-015-0068-x.
55. Moher, D., Liberati, A., Tetzlaff, J., et al., "Preferred Reporting Items for Systematic Reviews and Meta-Analyses: The PRISMA Statement", PLOS Medicine, **6**(7), pp. e1000097 (2009). DOI: 10.1371/journal.pmed.1000097.
56. Anwar, S.M., Majid, M., Qayyum, A., et al., "Medical Image Analysis using Convolutional Neural Networks: A Review", Journal of Medical Systems, **42**(11), pp. 226 (2018). DOI: 10.1007/s10916-018-1088-1.

57. Hoseini, F., Shahbahrami, A., and Bayat, P., "An efficient implementation of deep convolutional neural networks for MRI segmentation", Journal of digital imaging, **31**, pp. 738-747 (2018). DOI: 10.1007/s10278-018-0062-2.
58. Hoseini, F., Shahbahrami, A., and Bayat, P., "An Efficient Implementation of Deep Convolutional Neural Networks for MRI Segmentation", Journal of digital imaging, **31**(5), pp. 738-747 (2018). DOI: 10.1007/s10278-018-0062-2.
59. Naser, M.A., and Deen, M.J., "Brain tumor segmentation and grading of lower-grade glioma using deep learning in MRI images", Computers in Biology and Medicine, 121, pp. 103758 (2020). DOI: 10.1016/j.compbiomed.2020.103758.
60. Bangalore Yogananda, C.G., Wagner, B., Nalawade, S.S., et al., "Fully Automated Brain Tumor Segmentation and Survival Prediction of Gliomas Using Deep Learning and MRI", Brainlesion: Glioma, Multiple Sclerosis, Stroke and Traumatic Brain Injuries, Springer International Publishing, Cham, pp. 99-112 (2020). DOI: 10.1101/760157.
61. Banerjee, S., and Mitra, S., "Novel Volumetric Sub-region Segmentation in Brain Tumors", Frontiers in Computational Neuroscience, **14**(3) (2020). DOI: 10.3389/fncom.2020.00003.
62. Feng, X., Tustison, N.J., Patel, S.H., and Meyer, C.H., "Brain tumor segmentation using an ensemble of 3d u-nets and overall survival prediction using radiomic features", Frontiers in computational neuroscience, **14**, pp. 25 (2020). DOI: 10.3389/fncom.2020.00025.
63. Munir, K., Frezza, F., and Rizzi, A., *Brain Tumor Segmentation Using 2D-UNET Convolutional Neural Network*, in *Deep Learning for Cancer Diagnosis*, U. Kose and J. Alzubi, Editors. 2021, Springer Singapore: Singapore. p. 239-248. DOI: 10.1007/978-981-15-6321-8.
64. McHugh, H., Talou, G.M., and Wang, A., "2D Dense-UNet: A Clinically Valid Approach to Automated Glioma Segmentation", Brainlesion: Glioma, Multiple Sclerosis, Stroke and Traumatic Brain Injuries: 6th International Workshop, BrainLes 2020, Held in Conjunction with MICCAI 2020, Lima, Peru, October 4, 2020, Revised Selected Papers, Part II, Springer Nature, pp. 69 (2021). DOI: 10.1007/978-3-030-72087-2_7.
65. Kaldera, H., Gunasekara, S.R., and Dissanayake, M.B., "MRI based Glioma segmentation using Deep Learning algorithms", 2019 International Research Conference on Smart Computing and Systems Engineering (SCSE), pp. 51-56 (2019). DOI: 10.23919/SCSE.2019.8842668.
66. Tripathi, S., Verma, A., and Sharma, N., "Automatic segmentation of brain tumour in MR images using an enhanced deep learning approach", Computer Methods in Biomechanics and Biomedical Engineering: Imaging & Visualization, **9**(2), pp. 121-130 (2021). DOI: 10.1109/ACCESS.2023.3288017.
67. Yeung, M., Sala, E., Schönlieb, C.-B., and Rundo, L., "A mixed focal loss function for handling class imbalanced medical image segmentation", arXiv preprint arXiv:2102.04525, (2021). DOI: 10.48550/arXiv.2102.04525.
68. Liu, J., Liu, H., Tang, Z., et al., "IOUC-3DSFCNN: Segmentation of Brain Tumors via IOU Constraint 3D Symmetric Full Convolution Network with Multimodal Auto-context", Scientific Reports, **10**(1), pp. 6256 (2020). DOI: 10.1038/s41598-020-63242-x.
69. Kao, P.-Y., Shailja, F., Jiang, J., et al., "Improving patch-based convolutional neural networks for MRI brain tumor segmentation by leveraging location information", Frontiers in neuroscience, **13**, pp. 1449 (2020). DOI: 10.3389/fnins.2019.01449.
70. Ellison, J.C., *Improving the generalizability of convolutional neural networks for brain tumor segmentation in the post-treatment setting*. 2020, UCSF. DOI: 10.48550/arXiv.1907.01268.
71. Grivalsky, S., Tamajka, M., and Benesova, W., "Segmentation of gliomas in magnetic resonance images using recurrent neural networks", 2019 42nd International Conference on Telecommunications and Signal Processing (TSP), IEEE, pp. 539-542 (2019). DOI: 10.1109/TSP.2019.8769056.
72. SivaSai, J.G., Srinivasu, P.N., Sindhuri, M.N., et al., *An Automated Segmentation of Brain MR Image through Fuzzy Recurrent Neural Network*, in *Bio-inspired Neurocomputing*. 2021, Springer. p. 163-179. DOI: 10.1007/978-981-15-5495-7_9.
73. Nema, S., Dudhane, A., Murala, S., and Naidu, S., "RescueNet: An unpaired GAN for brain tumor segmentation", Biomedical Signal Processing and Control, **55**, pp. 101641 (2020). DOI: 10.1016/j.bspc.2019.101641.
74. Mecheter, I., Amira, A., Abbod, M., and Zaidi, H., "Brain MR Imaging Segmentation Using Convolutional Auto Encoder Network for PET Attenuation Correction", Proceedings of SAI Intelligent Systems Conference, Springer, pp. 430-440 (2020). DOI: 10.1007/978-3-030-55190-2_32.
75. McKinley, R., Rebsamen, M., Meier, R., and Wiest, R., "Triplanar ensemble of 3d-to-2d cnns with label-uncertainty for brain tumor segmentation", International MICCAI Brainlesion Workshop, Springer, pp. 379-387 (2019). DOI: 10.1007/978-3-030-46640-4_36.
76. Wang, G., Li, W., Zuluaga, M.A., et al., "Interactive Medical Image Segmentation Using Deep Learning With Image-Specific Fine Tuning", IEEE Transactions on Medical Imaging, **37**(7), pp. 1562-1573 (2018). DOI: 10.1109/TMI.2018.2791721.
77. Wang, G., Zuluaga, M.A., Li, W., et al., "DeepIGeoS: a deep interactive geodesic framework for medical image segmentation", IEEE transactions on pattern analysis and machine intelligence, **41**(7), pp. 1559-1572 (2018). DOI: 10.1109/TPAMI.2018.2840695.

78. Sung, H., Ferlay, J., Siegel, R.L., et al., "Global cancer statistics 2020: GLOBOCAN estimates of incidence and mortality worldwide for 36 cancers in 185 countries", CA: a cancer journal for clinicians, **71**(3), pp. 209-249 (2021). DOI: 10.3322/caac.21660.
79. Van Ginneken, B., Heimann, T., and Styner, M., "3D segmentation in the clinic: A grand challenge", MICCAI workshop on 3D segmentation in the clinic: a grand challenge, pp. 7-15 (2007).
80. Valindria, V.V., Pawlowski, N., Rajchl, M., et al., "Multi-modal learning from unpaired images: Application to multi-organ segmentation in CT and MRI", 2018 IEEE winter conference on applications of computer vision (WACV), IEEE, pp. 547-556 (2018). DOI: 10.1109/WACV.2018.00066.
81. Chaunzwa, T.L., Hosny, A., Xu, Y., et al., "Deep learning classification of lung cancer histology using CT images", Scientific Reports, **11**(1), pp. 5471 (2021). DOI: 10.1038/s41598-021-84630-x.
82. Jalali, Y., Fateh, M., Rezvani, M., et al., "ResBCDU-Net: A Deep Learning Framework for Lung CT Image Segmentation", Sensors, **21**(1) (2021). DOI: 10.3390/s21010268.
83. Díaz-Pernas, F.J., Martínez-Zarzuela, M., Antón-Rodríguez, M., and González-Ortega, D., "A Deep Learning Approach for Brain Tumor Classification and Segmentation Using a Multiscale Convolutional Neural Network", Healthcare, **9**(2), pp. 153 (2021). DOI: 10.3390/healthcare9020153.
84. Zhang, W., Yang, G., Huang, H., et al., "ME-Net: Multi-encoder net framework for brain tumor segmentation", International Journal of Imaging Systems and Technology, pp. 1834–1848 (2021). DOI: 10.1002/ima.22571.
85. Aswani, K., and Menaka, D., "A dual autoencoder and singular value decomposition based feature optimization for the segmentation of brain tumor from MRI images", BMC Medical Imaging, **21**(1), pp. 82 (2021). DOI: 10.1186/s12880-021-00614-3.
86. Zhou, X., Li, X., Hu, K., et al., "ERV-Net: An efficient 3D residual neural network for brain tumor segmentation", Expert Systems with Applications, 170, pp. 114566 (2021). DOI: 10.1016/j.eswa.2021.114566.
87. Ahmad, P., Jin, H., Qamar, S., et al., "RD2A: densely connected residual networks using ASPP for brain tumor segmentation", Multimedia Tools and Applications, (2021). DOI: 10.1007/s11042-021-10915-y.
88. Cirillo, M.D., Abramian, D., and Eklund, A., "Vox2Vox: 3D-GAN for brain tumour segmentation", arXiv preprint arXiv:2003.13653, (2020). DOI: /10.48550/arXiv.2003.13653.
89. Ben naceur, M., Akil, M., Saouli, R., and Kachouri, R., "Fully automatic brain tumor segmentation with deep learning-based selective attention using overlapping patches and multi-class weighted cross-entropy", Medical Image Analysis, **63**, pp. 101692 (2020). DOI: 10.1016/j.media.2020.101692.
90. Bangalore Yogananda, C.G., Shah, B.R., Vejdani-Jahromi, M., et al., "A Fully Automated Deep Learning Network for Brain Tumor Segmentation", Tomography (Ann Arbor, Mich.), **6**(2), pp. 186-193 (2020). DOI: 10.18383/j.tom.2019.00026.
91. Aboelenein, N.M., Songhao, P., Koubaa, A., et al., "HTTU-Net: Hybrid Two Track U-Net for Automatic Brain Tumor Segmentation", IEEE Access, **8**, pp. 101406-101415 (2020). DOI: 10.1109/ACCESS.2020.2998601.
92. Chen, H., Qin, Z., Ding, Y., et al., "Brain tumor segmentation with deep convolutional symmetric neural network", Neurocomputing, **392**, pp. 305-313 (2020). DOI: 10.1016/j.neucom.2019.01.111.
93. Aziz, M.J., Zade, A.A.T., Farnia, P., et al., "Accurate automatic glioma segmentation in brain MRI images based on CapsNet", 2021 43rd Annual International Conference of the IEEE Engineering in Medicine & Biology Society (EMBC), IEEE, pp. 3882-3885 (2021). DOI: 10.1109/EMBC46164.2021.9630324.
94. Munir, K., Frezza, F., and Rizzi, A., "Deep Learning Hybrid Techniques for Brain Tumor Segmentation", Sensors, **22**(21), pp. 8201 (2022). DOI: 10.3390/s22218201.
95. Ottom, M.A., Rahman, H.A., and Dinov, I.D., "Znet: deep learning approach for 2D MRI brain tumor segmentation", IEEE Journal of Translational Engineering in Health and Medicine, **10**, pp. 1-8 (2022). DOI: 10.1109/JTEHM.2022.3176737.
96. Chang, Y., Zheng, Z., Sun, Y., et al., "Dpafnet: A residual dual-path attention-fusion convolutional neural network for multimodal brain tumor segmentation", Biomedical Signal Processing and Control, **79**, pp. 104037 (2023). DOI: 10.1016/j.bspc.2022.104037.
97. Moccia, S., De Momi, E., El Hadji, S., and Mattos, L.S., "Blood vessel segmentation algorithms—review of methods, datasets and evaluation metrics", Computer methods and programs in biomedicine, **158**, pp. 71-91 (2018). DOI: 10.1016/j.cmpb.2018.02.001.
98. Goni, M.R., Ruhaiyem, N.I.R., Mustapha, M., et al., "Brain vessel segmentation using deep learning-a review", IEEE Access, (2022). DOI: 10.1109/ACCESS.2022.3214987.
99. Xiao, X., Zhao, J., Qiang, Y., et al., "Radiomics-guided GAN for segmentation of liver tumor without contrast agents", International Conference on Medical Image Computing and Computer-Assisted Intervention, Springer, pp. 237-245 (2019). DOI: 10.1007/978-3-030-32245-8_27.
100. Lei, T., Wang, R., Zhang, Y., et al., "DefED-Net: Deformable Encoder-Decoder Network for Liver and Liver Tumor Segmentation", (2021). DOI: 10.1109/TRPMS.2021.3059780.

101. Zhang, Y., Pan, X., Li, C., and Wu, T., "3D liver and tumor segmentation with CNNs based on region and distance metrics", Applied Sciences, **10**(11), pp. 3794 (2020). DOI: 10.3390/app10113794
102. Chen, L., Song, H., Wang, C., et al., "Liver tumor segmentation in CT volumes using an adversarial densely connected network", BMC bioinformatics, **20**(16), pp. 1-13 (2019). DOI: 10.1186/s12859-019-3069-x.
103. Yuan, Y., "Hierarchical convolutional-deconvolutional neural networks for automatic liver and tumor segmentation", arXiv preprint arXiv:1710.04540, (2017). DOI: 10.48550/arXiv.1710.04540.
104. Albishri, A.A., Shah, S.J.H., and Lee, Y., "CU-Net: Cascaded U-Net model for automated liver and lesion segmentation and summarization", 2019 IEEE International Conference on Bioinformatics and Biomedicine (BIBM), IEEE, pp. 1416-1423 (2019). DOI: 10.1109/BIBM47256.2019.8983266.
105. Bi, L., Kim, J., Kumar, A., and Feng, D., "Automatic liver lesion detection using cascaded deep residual networks", arXiv preprint arXiv:1704.02703, (2017). DOI: 10.48550/arXiv.1704.02703.
106. Wang, B., Yang, J., Ai, J., et al., "Accurate tumor segmentation via octave convolution neural network", Frontiers in Medicine, **8**, pp. 653913 (2021). DOI: 10.3389/fmed.2021.653913.
107. Ayalew, Y.A., Fante, K.A., and Mohammed, M.A., "Modified U-Net for liver cancer segmentation from computed tomography images with a new class balancing method", BMC Biomedical Engineering, **3**, pp. 1-13 (2021). DOI: 10.1186/s42490-021-00050-y.
108. Rahman, H., Bukht, T.F.N., Imran, A., et al., "A Deep Learning Approach for Liver and Tumor Segmentation in CT Images Using ResUNet", Bioengineering, **9**(8), pp. 368 (2022). DOI: 10.3390/bioengineering9080368.
109. Balasubramanian, P.K., Lai, W.-C., Seng, G.H., and Selvaraj, J., "Apestnet with mask r-cnn for liver tumor segmentation and classification", Cancers, **15**(2), pp. 330 (2023). DOI: 10.3390/cancers15020330.
110. Baek, S., He, Y., Allen, B.G., et al., "Deep segmentation networks predict survival of non-small cell lung cancer", Scientific Reports, **9**(1), pp. 17286 (2019). DOI: 10.1038/s41598-019-53461-2.
111. Kasinathan, G., Jayakumar, S., Gandomi, A.H., et al., "Automated 3-D lung tumor detection and classification by an active contour model and CNN classifier", Expert Systems with Applications, 134, pp. 112-119 (2019). DOI: 10.1016/j.eswa.2019.05.041.
112. Dutta, K., "Densely Connected Recurrent Residual (Dense R2UNet) Convolutional Neural Network for Segmentation of Lung CT Images", arXiv preprint arXiv:2102.00663, (2021). DOI: 10.48550/arXiv.2102.00663.
113. Yamunadevi, M.M., and Ranjani, S.S., "Efficient segmentation of the lung carcinoma by adaptive fuzzy–GLCM (AF-GLCM) with deep learning based classification", Journal of Ambient Intelligence and Humanized Computing, **12**(5), pp. 4715-4725 (2021). DOI: 10.1007/s12652-020-01874-7.
114. Fu, X., Bi, L., Kumar, A., et al., "Multimodal Spatial Attention Module for Targeting Multimodal PET-CT Lung Tumor Segmentation", IEEE Journal of Biomedical and Health Informatics, pp. 1-1 (2021). DOI: 10.1109/JBHI.2021.3059453.
115. Nishio, M., Fujimoto, K., Matsuo, H., et al., "Lung cancer segmentation with transfer learning: usefulness of a pretrained model constructed from an artificial dataset generated using a generative adversarial network", Frontiers in Artificial Intelligence, **4**, pp. 694815 (2021). DOI: 10.3389/frai.2021.694815.
116. Chiu, T.-W., Tsai, Y.-L., and Su, S.-F., "Automatic detect lung node with deep learning in segmentation and imbalance data labeling", Scientific Reports, **11**(1), pp. 11174 (2021). DOI: 10.1038/s41598-021-90599-4.
117. Zhang, G., Yang, Z., and Jiang, S., "Automatic lung tumor segmentation from CT images using improved 3D densely connected UNet", Medical & Biological Engineering & Computing, **60**(11), pp. 3311-3323 (2022). DOI: 10.1007/s11517-022-02667-0.
118. Janowczyk, A., and Madabhushi, A., "Deep learning for digital pathology image analysis: A comprehensive tutorial with selected use cases", Journal of pathology informatics, **7** (2016). DOI: 10.4103/2153-3539.186902.
119. Wang, S., Chen, A., Yang, L., et al., "Comprehensive analysis of lung cancer pathology images to discover tumor shape and boundary features that predict survival outcome", Scientific reports, **8**(1), pp. 1-9 (2018). DOI: 10.1038/s41598-018-27707-4.
120. Roux, L., Racoceanu, D., Loménie, N., et al., "Mitosis detection in breast cancer histological images An ICPR 2012 contest", Journal of pathology informatics, **4** (2013). DOI: 10.4103/2153-3539.112693.
121. Cireşan, D.C., Giusti, A., Gambardella, L.M., and Schmidhuber, J., "Mitosis detection in breast cancer histology images with deep neural networks", International conference on medical image computing and computer-assisted intervention, Springer, pp. 411-418 (2013). DOI: 10.1007/978-3-642-40763-5_51.
122. Lal, S., Das, D., Alabhya, K., et al., "NucleiSegNet: Robust deep learning architecture for the nuclei segmentation of liver cancer histopathology images", Computers in Biology and Medicine, **128**, pp. 104075 (2021). DOI: 10.1016/j.compbiomed.2020.104075.
123. Serag, A., Ion-Margineanu, A., Qureshi, H., et al., "Translational AI and deep learning in diagnostic pathology", Frontiers in medicine, **6**, pp. 185 (2019). DOI: 10.3389/fmed.2019.00185.

124. Livne, M., Rieger, J., Aydin, O.U., et al., "A U-Net deep learning framework for high performance vessel segmentation in patients with cerebrovascular disease", Frontiers in neuroscience, **13**, pp. 97 (2019). DOI: 10.3389/fnins.2019.00097.
125. Yan, Q., Wang, B., Zhang, W., et al., "Attention-guided deep neural network with multi-scale feature fusion for liver vessel segmentation", IEEE Journal of Biomedical and Health Informatics, **25**(7), pp. 2629-2642 (2020). DOI: 10.1109/JBHI.2020.3042069.
126. Su, J., Liu, Z., Zhang, J., et al., "DV-Net: Accurate liver vessel segmentation via dense connection model with D-BCE loss function", Knowledge-Based Systems, **232**, pp. 107471 (2021). DOI: 10.1016/j.knosys.2021.107471.
127. Survarachakan, S., Pelanis, E., Khan, Z.A., et al., "Effects of enhancement on deep learning based hepatic vessel segmentation", Electronics, **10**(10), pp. 1165 (2021). DOI: 10.3390/electronics10101165.
128. Yang, J., Fu, M., and Hu, Y., "Liver vessel segmentation based on inter-scale V-Net", Math. Biosci. Eng, **18**(4), pp. 4327-40 (2021). DOI: 10.3934/mbe.2021217.
129. Meng, X., Zhang, X., Wang, G., et al., "Exploiting full resolution feature context for liver tumor and vessel segmentation via fusion encoder: Application to liver tumor and vessel 3D reconstruction", arXiv preprint arXiv:2111.13299, (2021). DOI: 10.48550/arXiv.2111.13299.
130. Wu, M., Qian, Y., Liao, X., et al., "Hepatic vessel segmentation based on 3D swin-transformer with inductive biased multi-head self-attention", BMC Medical Imaging, **23**(1), pp. 1-14 (2023). DOI: 10.1186/s12880-023-01045-y.
131. Alirr, O.I., and Rahni, A.A.A., "Hepatic vessels segmentation using deep learning and preprocessing enhancement", Journal of applied clinical medical physics, **24**(5), pp. e13966 (2023). DOI: 10.1002/acm2.13966.
132. Gu, Z., Cheng, J., Fu, H., et al., "Ce-net: Context encoder network for 2d medical image segmentation", IEEE transactions on medical imaging, **38**(10), pp. 2281-2292 (2019). DOI: 10.1109/TMI.2019.2903562.
133. Xiao, X., Lian, S., Luo, Z., and Li, S., "Weighted Res-UNet for High-Quality Retina Vessel Segmentation", 2018 9th International Conference on Information Technology in Medicine and Education (ITME), pp. 327-331 (2018). DOI: 10.1109/ITME.2018.00080.
134. Zahangir Alom, M., Hasan, M., Yakopcic, C., et al., "Recurrent Residual Convolutional Neural Network based on U-Net (R2U-Net) for Medical Image Segmentation", arXiv e-prints, pp. arXiv:1802.06955 (2018). DOI: 10.48550/arXiv.1802.06955.
135. Valanarasu, J.M.J., Sindagi, V.A., Hacihaliloglu, I., and Patel, V.M., "KiU-Net: Towards Accurate Segmentation of Biomedical Images Using Over-Complete Representations", Medical Image Computing and Computer Assisted Intervention – MICCAI 2020, Springer International Publishing, Cham, pp. 363-373 (2020). DOI: 10.1007/978-3-030-59719-1_36.
136. Fu, H., Xu, Y., Lin, S., et al., "DeepVessel: Retinal Vessel Segmentation via Deep Learning and Conditional Random Field", Medical Image Computing and Computer-Assisted Intervention – MICCAI 2016, Springer International Publishing, Cham, pp. 132-139 (2016). DOI: 10.1007/978-3-319-46723-8_16.
137. Yan, Z., Yang, X., and Cheng, K.T., "Joint Segment-Level and Pixel-Wise Losses for Deep Learning Based Retinal Vessel Segmentation", IEEE Transactions on Biomedical Engineering, **65**(9), pp. 1912-1923 (2018). DOI: 10.1109/TBME.2018.2828137.
138. Jiang, Z., Zhang, H., Wang, Y., and Ko, S.-B., "Retinal blood vessel segmentation using fully convolutional network with transfer learning", Computerized Medical Imaging and Graphics, 68, pp. 1-15 (2018). DOI: 10.1016/j.compmedimag.2018.04.005.
139. Noh, K.J., Park, S.J., and Lee, S., "Scale-space approximated convolutional neural networks for retinal vessel segmentation", Computer Methods and Programs in Biomedicine, 178, pp. 237-246 (2019). DOI: 10.1016/j.cmpb.2019.06.030.
140. Jiang, Y., Wang, F., Gao, J., and Liu, W., "Efficient BFCN for automatic retinal vessel segmentation", Journal of Ophthalmology, **2020** (2020). DOI: 10.1155/2020/6439407.
141. Wang, D., Haytham, A., Pottenburgh, J., et al., "Hard Attention Net for Automatic Retinal Vessel Segmentation", IEEE Journal of Biomedical and Health Informatics, **24**(12), pp. 3384-3396 (2020). DOI: 10.1109/JBHI.2020.3002985.
142. Ma, Y., Li, X., Duan, X., et al., "Retinal Vessel Segmentation by Deep Residual Learning with Wide Activation", Computational Intelligence and Neuroscience, **2020** (2020). DOI: 10.1155/2020/8822407.
143. Al-Masni, M.A., and Kim, D.-H., "CMM-Net: Contextual multi-scale multi-level network for efficient biomedical image segmentation", Scientific Reports, **11**(1), pp. 1-18 (2021). DOI: 10.1038/s41598-021-89686-3.
144. Liu, Y., Shen, J., Yang, L., et al., "ResDO-UNet: A deep residual network for accurate retinal vessel segmentation from fundus images", Biomedical Signal Processing and Control, **79**, pp. 104087 (2023). DOI: 10.1016/j.bspc.2022.104087.
145. Oda, M., Roth, H.R., Kitasaka, T., et al., "Abdominal artery segmentation method from CT volumes using fully convolutional neural network", International Journal of Computer Assisted Radiology and Surgery, **14**(12), pp. 2069-2081 (2019). DOI: 10.1007/s11548-019-02062-5.

146. Mohammadi, S., Mohammadi, M., Dehlaghi, V., and Ahmadi, A., "Automatic Segmentation, Detection, and Diagnosis of Abdominal Aortic Aneurysm (AAA) Using Convolutional Neural Networks and Hough Circles Algorithm", Cardiovascular Engineering and Technology, **10**(3), pp. 490-499 (2019). DOI: 10.1007/s13239-019-00421-6.
147. Yang, S., Kweon, J., Roh, J.-H., et al., "Deep learning segmentation of major vessels in X-ray coronary angiography", Scientific reports, **9**(1), pp. 1-11 (2019). DOI: 10.1038/s41598-019-53254-7.
148. Fu, F., Wei, J., Zhang, M., et al., "Rapid vessel segmentation and reconstruction of head and neck angiograms using 3D convolutional neural network", Nature communications, **11**(1), pp. 1-12 (2020). DOI: 10.1038/s41467-020-18922-7.
149. Bar, Y., Diamant, I., Wolf, L., and Greenspan, H., "Deep learning with non-medical training used for chest pathology identification", Medical Imaging 2015: Computer-Aided Diagnosis, International Society for Optics and Photonics, pp. 94140V (2015). DOI: 10.1117/12.2083124.
150. Xu, J., Luo, X., Wang, G., et al., "A deep convolutional neural network for segmenting and classifying epithelial and stromal regions in histopathological images", Neurocomputing, **191**, pp. 214-223 (2016). DOI: 10.1016/j.neucom.2016.01.034.
151. Hermsen, M., de Bel, T., Den Boer, M., et al., "Deep learning–based histopathologic assessment of kidney tissue", Journal of the American Society of Nephrology, **30**(10), pp. 1968-1979 (2019). DOI: 10.1681/ASN.2019020144.
152. Jiménez, G., and Racoceanu, D., "Deep learning for semantic segmentation vs. classification in computational pathology: Application to mitosis analysis in breast cancer grading", Frontiers in bioengineering and biotechnology, **7**, pp. 145 (2019). DOI: 10.3389/fbioe.2019.00145.
153. Kurc, T., Bakas, S., Ren, X., et al., "Segmentation and classification in digital pathology for glioma research: Challenges and deep learning approaches", Frontiers in neuroscience, **14** (2020). DOI: 10.3389/fnins.2020.00027.
154. Conze, P.-H., Brochard, S., Burdin, V., et al., "Healthy versus pathological learning transferability in shoulder muscle MRI segmentation using deep convolutional encoder-decoders", Computerized Medical Imaging and Graphics, **83**, pp. 101733 (2020). DOI: 10.1016/j.compmedimag.2020.101733.
155. Huang, P., Tan, X., Chen, C., et al., "AF-SENet: Classification of Cancer in Cervical Tissue Pathological Images Based on Fusing Deep Convolution Features", Sensors, **21**(1), pp. 122 (2021). DOI: 10.3390/s21010122.
156. Khened, M., Kori, A., Rajkumar, H., et al., "A generalized deep learning framework for whole-slide image segmentation and analysis", Scientific reports, **11**(1), pp. 1-14 (2021). DOI: 10.1038/s41598-021-90444-8.
157. Hemelings, R., Elen, B., Blaschko, M.B., et al., "Pathological myopia classification with simultaneous lesion segmentation using deep learning", Computer Methods and Programs in Biomedicine, **199**, pp. 105920 (2021). DOI: 10.1016/j.cmpb.2020.105920.
158. Deng, R., Liu, Q., Cui, C., et al., "Single Dynamic Network for Multi-label Renal Pathology Image Segmentation", International Conference on Medical Imaging with Deep Learning, PMLR, pp. 304-314 (2022).

Tables and Figures List

Figure 9. Inclusion and exclusion criteria for selection of articles for systematic review according to the PRISMA guidance.

Table 1. Summary of DL approaches in brain tumor segmentation.

Table 2. Summary of DL approaches in liver tumor segmentation.

Table 3. Summary of DL approaches in lung tumor segmentation.

Table 4. Summary of DL approaches in blood vessel segmentation.

Table 5. Summary of DL approaches in pathology image segmentation.

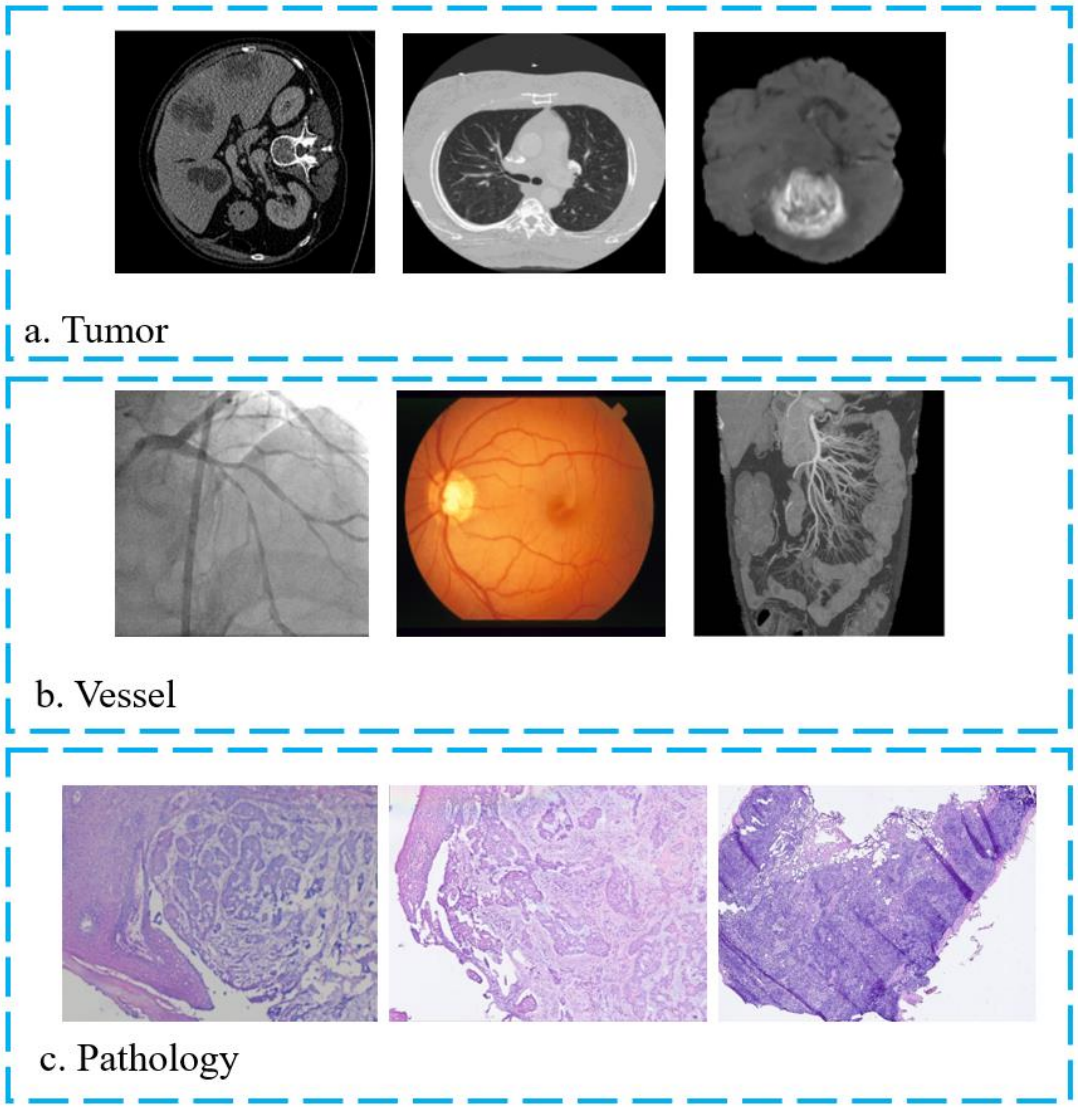

Figure 1. Visualization of three main groups of targets including tumor [20], vessel [21], and pathological images [22] for medical image segmentation.

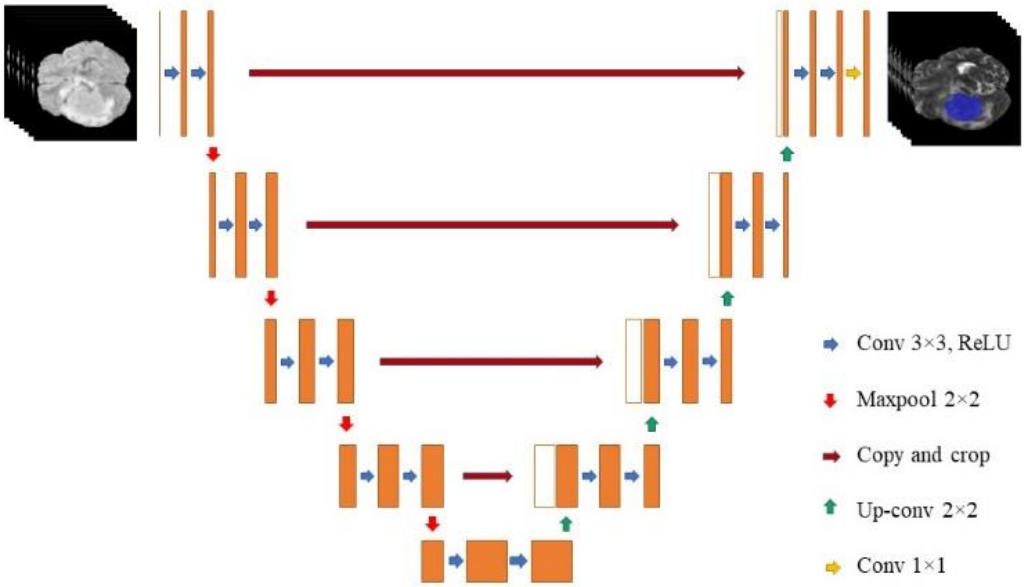

Figure 2.

U-Net architecture.

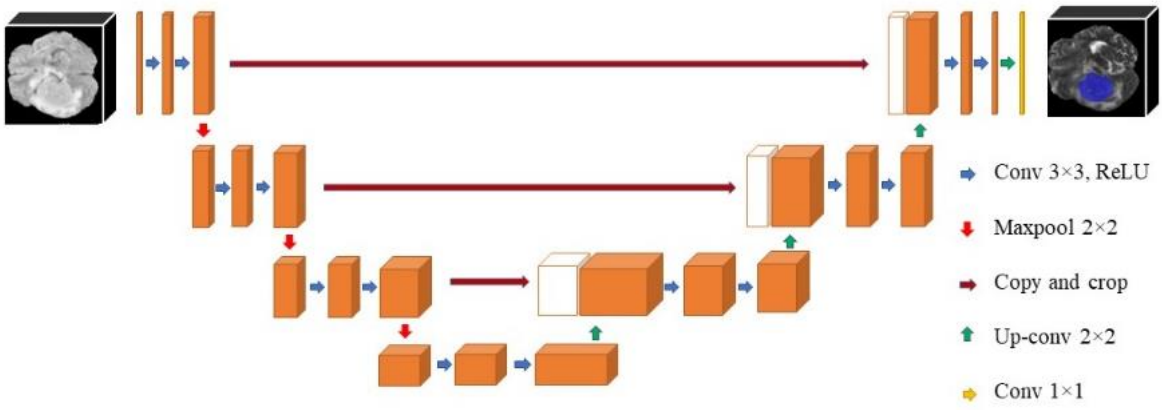

Figure 3.

3D U-Net architectur e [25].

Figure 4.

GAN architecture .

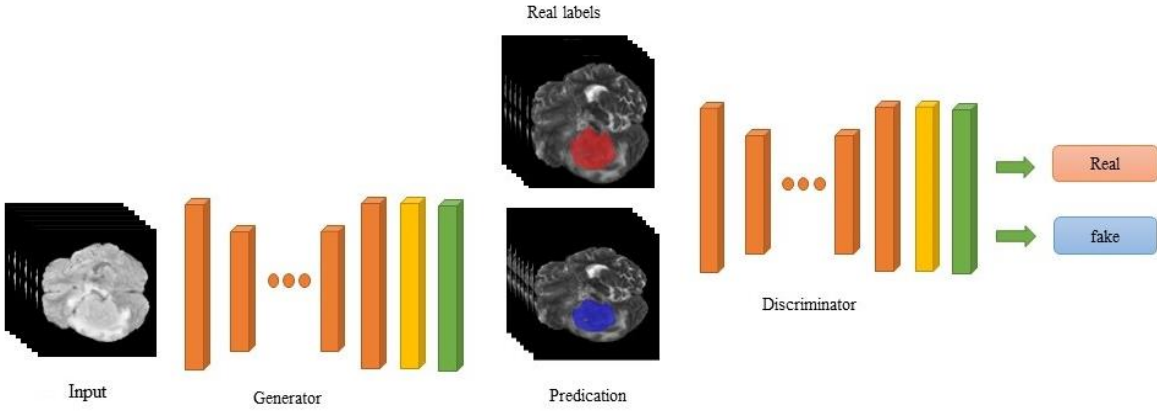

Figure 5.

RNN architecture.

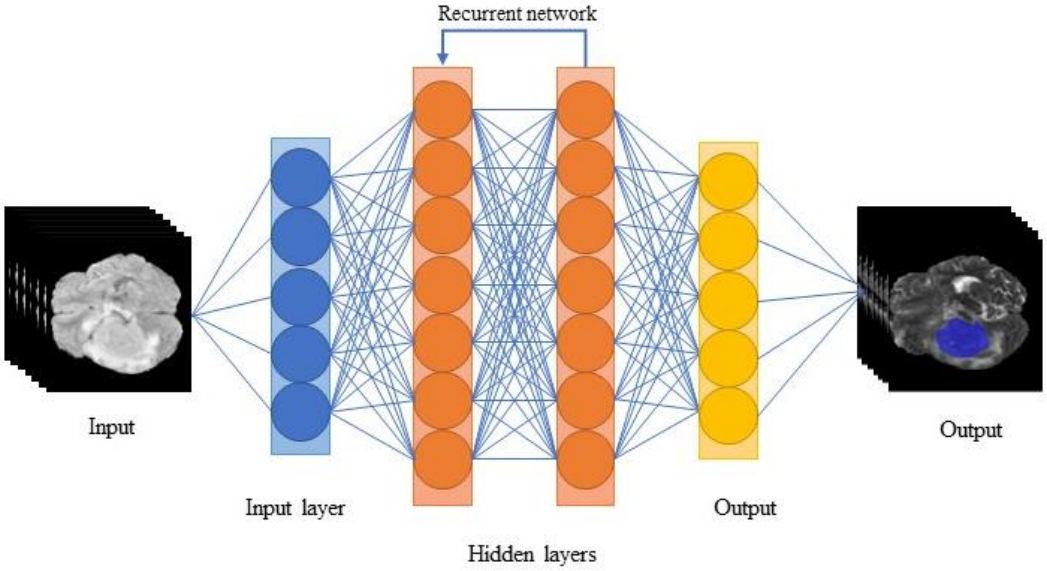

Figure 6.

AE-based DL architecture.

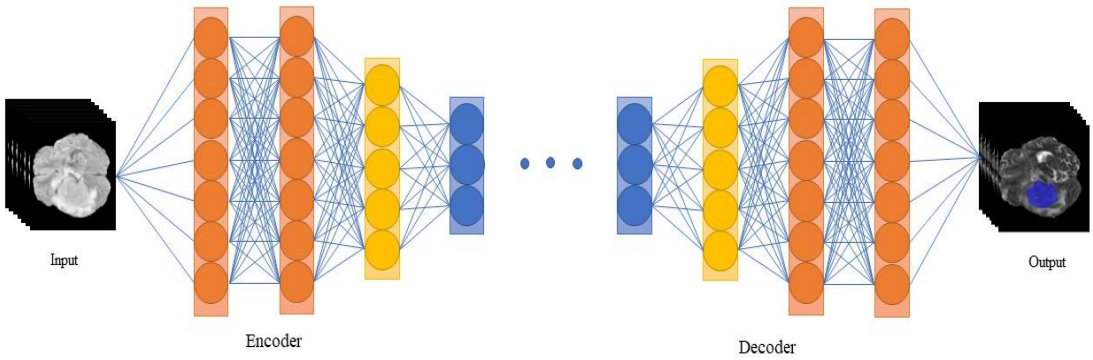

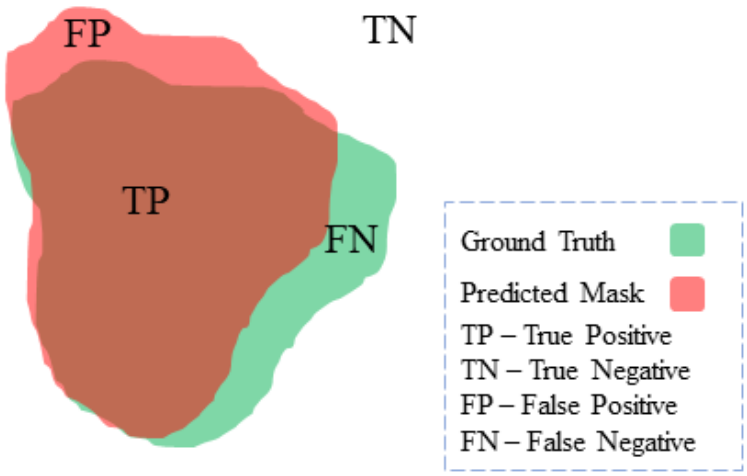

Figure 7. Schematic illustration of four basic error rate definitions.

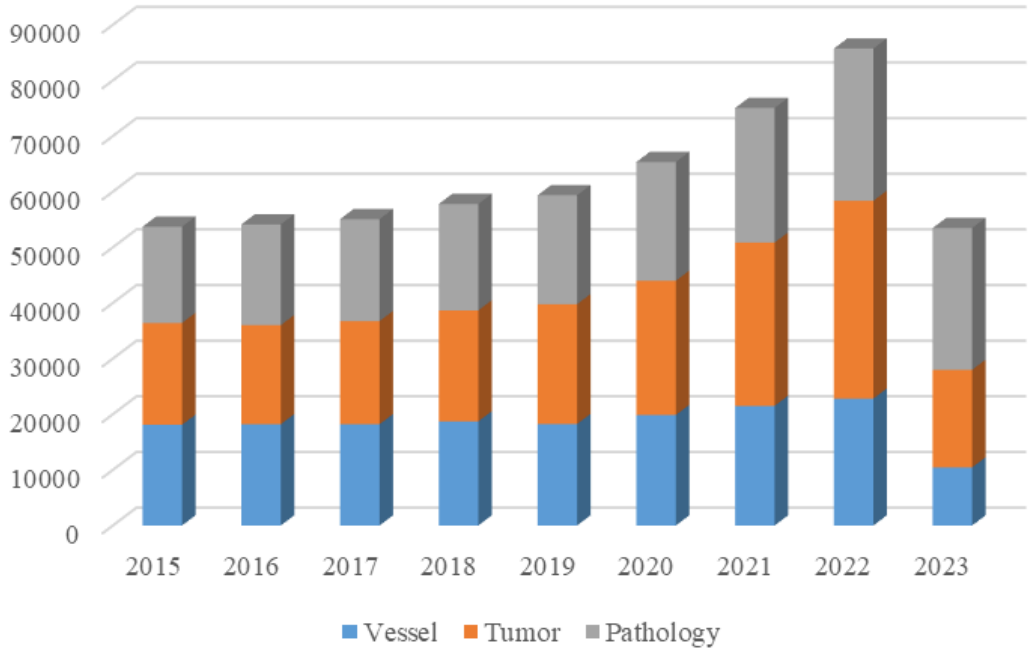

Figure 8. The number of publications for target-based segmentation (till April 2023).

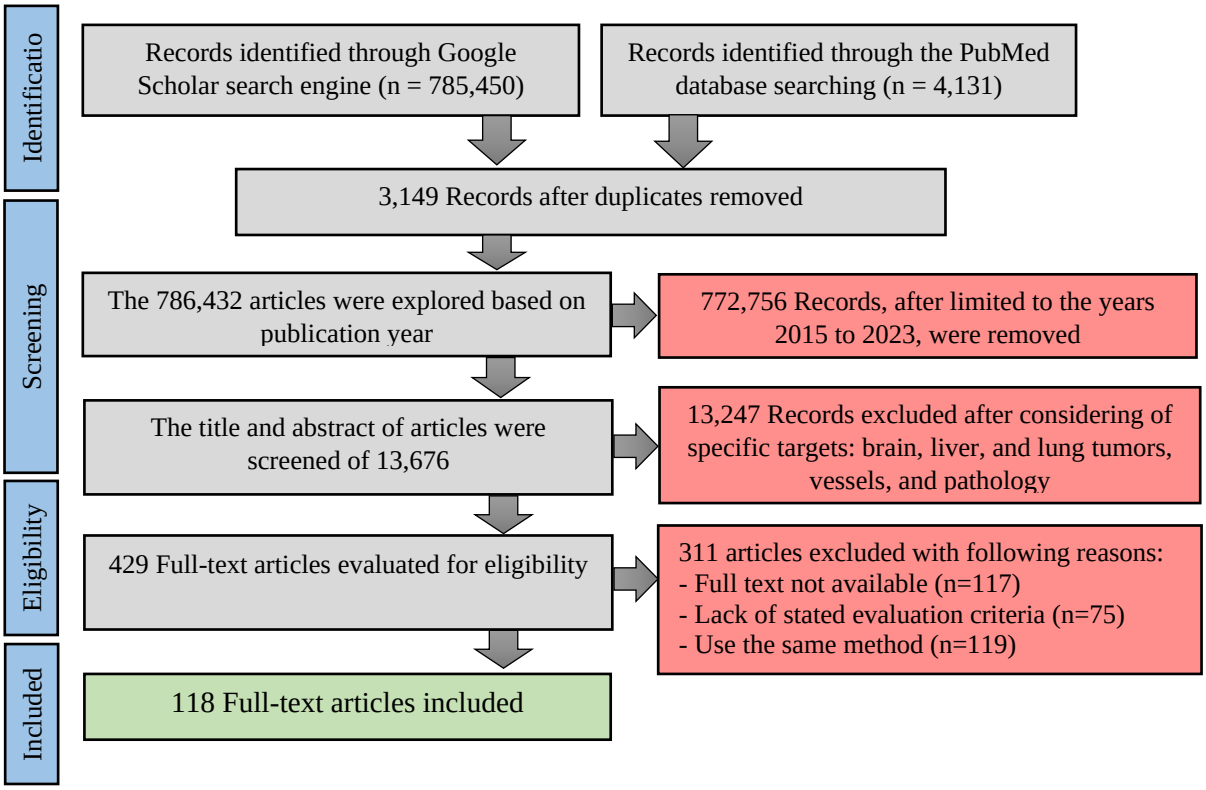

Figure 9. Inclusion and exclusion criteria for selection of articles for systematic review according to the PRISMA guidance.

Table 1. Summary of DL approaches in brain tumor segmentation.

Ref	Organ/ modality	Method	Performance metrics			
			DSC	***TPR***	***TNR***	***ACC***
[83]	Brain MRI image	***Network arch:*** *CNN* ***Approach:*** Image processing in 3 spatial scales ***Dataset:*** BraTS2015	0.82	0.94	-	-
[84]		***Network arch:*** CNN ***Approach:*** "Categorical Dice" loss function ***Dataset:*** BraTS2020	0.88	-	-	-
[85]		***Network arch:*** Auto-encoder ***Approach:*** latent space optimization ***Dataset:*** BraTS2015	0.84	0.89	-	-
[86]		***Network arch:*** Residual net ***Approach:*** A fusion of Dice loss & cross-entropy loss, introducing a computation-efficient network ***Dataset:*** BraTS2018	0.91	-	-	-
[87]		***Network arch:*** Residual net ***Approach:*** A combination of the residual connections, dilation, and dense Atrous-Spatial Pyramid Pooling to preserve more contextual information ***Dataset:*** BraTS2019	0.90	-	-	-
[88]		***Network arch:*** GAN ***Approach:*** 3D volume-to-volume Generative Adversarial Network ***Dataset:*** BraTS2020	0.87	-	-	-
[89]		***Network arch:*** CNN	0.90	-	-	-

		Approach: Using the selective attention technique ***Dataset:*** BraTS2018				
[90]		***Network arch:*** 3D-Dense-UNets ***Approach:*** Designed three separate 3D-Dense-UNets to simplify the complex multiclass segmentation problem ***Dataset:*** BraTS2017 - BraTS2018	0.90	-	-	-
[91]		***Network arch:*** Hybrid Two Track U-Net ***Approach:*** Using hybrid networks, Leaky ReLU activation, and optimization of the loss function to address the class imbalance problem ***Dataset:*** BraTS2018	0.89	-	-	-
[92]		***Network arch:*** Hybrid Two Track U-Net ***Approach:*** Adding symmetric masks in several layers to improve segmentation results ***Dataset:*** BraTS2015	0.85	-	-	-
[93]		***Network arch:*** capsule network ***Approach:*** Use new networks to achieve high performance using less data ***Dataset:*** BraTS2020	0.87	-	-	-
[94]		***Network arch:*** MI-UNet ***Approach:*** Depth-wise separable Hybrid model ***Dataset:*** BraTS2019	0.87	0.90	0.99	-
[95]		***Network arch:*** Znet ***Approach:*** Z-net based on an encoder-decoder architecture, and data amplification to propagate the intrinsic affinities ***Dataset:*** TCGA - LGG	0.91	-	-	0.99
[96]		***Network arch:*** DPAFNet ***Approach:*** 3D segmentation model based on dual-path module and multi-scale attention fusion module ***Dataset:*** BraTS2018, BraTS2019 and, BraTS2020	0.89	-	-	-

Table 2. Summary of DL approaches in liver tumor segmentation.

Ref	**Organ/modality**	**Method**	**Performance metrics**			
			DSC	***TPR***	***TNR***	***ACC***
[99]	Liver / CT Image	***Network architecture:*** Radiomics-guided GAN ***Approach:*** The discriminator uses the radiomics feature from the contrast images as prior knowledge ***Dataset:*** LiTS17	0.92	---	---	---
[100]		***Network architecture:*** deformable encoder-decoder network (DefED-Net) ***Approach:*** Deformable convolution is used to enhance the feature representation capability of DefED-Net ***Dataset:*** LiTS and the 3DIRCADb	LiTS: 0.87 3DIRCADb: 0.66	---	---	---
[101]		***Network architecture:*** Improved V-net algorithm ***Approach:*** 3D liver and tumor segmentation based on three distance-based loss functions and the regional loss function jointly ***Dataset:*** LiTS17 and 3D-IRCADb	LiTS17: 0.764 3DIRCADb: 0.682	0.998 0.999	0.682 0.682	--- ---
[102]		***Network architecture:*** Adversarial densely connected network ***Approach:*** Develop a deep 3D densely connected fully CNN with an adversarial training strategy ***Dataset:*** LiTS17	0.68	---	---	---
[103]		***Network architecture:*** CDNN ***Approach:*** Liver histogram equalization, input to the CDNN for tumor segmentation. Jaccard distance is used as a loss function. ***Dataset:*** LiTS17	0.657	---	---	---
[104]		***Network architecture:*** Cascaded U-Net ***Approach:*** Cascaded U-Net model for automated liver and lesion segmentation ***Dataset:*** LiTS	0.59	---	---	---
[1]		***Network architecture:*** Spatial Feature Fusion Convolutional Network ***Approach:*** SFF-Net learns more spatial information by adding skip connections and feature fusion blocks ***Dataset:*** LiTS17	0.59	---	---	---
[105]		***Network architecture:*** ResNet	0.500	---	---	---

		Approach: Novel cascaded ResNet architecture with multi-scale fusion ***Dataset:*** LiTS17				
[106]		***Network architecture:*** Octave CNN ***Approach:*** Learning multiple-spatial-frequency features ***Dataset:*** LiTS	0.96	---	---	0.95
[107]		***Network architecture:*** Modified U-Net ***Approach:*** Class balancing method ***Dataset:*** LiTS	0.74	---	---	---
[108]		***Network architecture:*** Hybrid ResUNet ***Approach:*** Combining the ResNet and UNet models ***Dataset:*** IRCADB01	0.99	---	---	0.99
[109]		***Network architecture:*** Enhanced Swin Transformer Network with Adversarial Propagation ***Approach:*** Enhanced mask region-based CNN model then segmented picture is fed onto an Enhanced Swin Transformer Network with Adversarial Propagation ***Dataset:*** LiTS17 and SLiver073	---	---	---	0.94

Table 3. Summary of DL approaches in lung tumor segmentation.

Ref	**Organ/ modality**	**Method**	**Performance metrics (Mean ± std)**			
			DSC	***TPR***	***TNR***	***ACC***
[110]	NSCLC / CT	***Network architecture:*** The U-Net ***Approach:*** "Bottleneck Layer" to compress image features ***Dataset:*** PET-CT images of 96 NSCLC patients	0.86± 0.03	---	---	---
	NSCLC / PET		0.82± 0.08	---	---	---
[111]	Nodule / CT	***Network architecture:*** CNN with the active contour model (ACM) ***Approach:*** Enhanced CNN algorithm (E-CNN) with AlexNet layer ***Dataset:*** 311 early-stage NSCLC patients	---	0.95	0.91	0.97
[81]	NSCLC / CT	***Network architecture:*** The VGG-16 ***Approach:*** Machine learning classifiers on CNN ***Dataset:*** 311 early-stage NSCLC patients	---	---	---	---
[112]	Nodule / CT	***Network architecture:*** The Dense R2U CNN ***Approach:*** Using layers of recurrent, residual, convolutional, and dense interconnections ***Dataset:*** LUNA	0.98 ± 0.009	0.99 ± 0.002	0.98 ± 0.02	0.99 ± 0.003
[113]	Carcinoma / Bronchoscopy	***Network architecture:*** The CNN ***Approach:*** Adaptive fuzzy-GLCM + GoogLeNet ***Dataset:*** 200 images of Hamlyn lung and bronchoscopy	---	0.98	0.98	0.98
[114]	STS / PET-CT	***Network architecture:*** The U-Net ***Approach:*** Multimodal Spatial Attention Module (MSAM) ***Dataset:*** NSCLC and STS	***NSCLC Dataset***			
			0.71	0.81	0.99	---
			STS Dataset			
			0.62	0.64	0.99	---
[82]	Lung Cancer / CT	***Network architecture:*** The ResBCDU-Net ***Approach:*** The BConvLSTM as an integrator module ***Dataset:*** LIDC-IDRI	0.97	0.97	---	0.97
[115]	Lung Cancer / CT	***Network architecture:*** The GAN ***Approach:*** Transfer learning ***Dataset:*** LUNA16	0.72	---	---	---
[116]	Lung Cancer / CT	***Network architecture:*** The 2D U-net ***Approach:*** Using a 2D UNet network with imbalance data labeling ***Dataset:*** 472 cases of TMUH clinical data	0.79	---	---	---
[117]	Lung Cancer / CT	***Network architecture:*** DenseUNet ***Approach:*** Aims to contribute similar feature maps between encoder and decoder sub-networks ***Dataset:*** TCIA and LIDC	0.83	---	---	0.97

Table 4. Summary of DL approaches in blood vessel segmentation.

Ref	Organ/ modality	Method	Performance metrics			
			DSC	***TPR***	***TNR***	***ACC***
[124]	Brain / MRI	***Network architecture:*** The U-Net CNN model ***Approach:*** "Half U-Net" ***Dataset:*** PEGASUS study	0.88	---	---	---
[125]	Liver/ 3Phasic CT	***Network architecture:*** The LVSNet model ***Approach:*** Attention-Guided Deep Neural Network with Multi-Scale Feature Fusion ***Dataset:*** MSD	0.90	---	---	---
[126]		***Network architecture:*** The DV-Net model ***Approach:*** Segmentation via dense connection model with D-BCE loss function ***Dataset:*** MSD	0.75	---	---	---
[127]		***Network architecture:*** The 3D U-net model ***Approach:*** Effect of enhancement on segmentation using a deep learning model ***Dataset:*** 57 cases from Oslo University hospital	0.80	---	---	---
[128]		***Network architecture:*** The 3D V-net model ***Approach:*** Using inter-scale dense connections and high-level semantic information ***Dataset:*** 3Dircadb	0.71	---	---	---
[129]		***Network architecture:*** The TransFusionNet model ***Approach:*** A multi-scale feature fusion network ***Dataset:*** 3Dircadb	0.92	---	---	---
[130]		***Network architecture:*** IBIMHAV-Net ***Approach:*** Expanding the swing transformer to 3D and employing an effective combination of convolution and self-attention ***Dataset:*** 3Dircadb	0.74	0.77	---	---
[131]		***Network architecture:*** U-Net ***Approach:*** Modified residual block to include concatenation skip connection ***Dataset:*** MSD	0.79	---	---	---
[132]	Retinal/ OCT	***Network architecture:*** The CE-Net model ***Approach:*** Using blocks of ResNet, dense atrous convolution, and residual multi-kernel pooling ***Dataset:*** DRIVE and TOPCON	---	0.83	---	0.95
[133]	Retinal / Ophthalmoscope	***Network architecture:*** The Weighted ResUNet model ***Approach:*** The binary cross-entropy loss function ***Dataset:*** DRIVE and STARE	***DRIVE dataset***			
			---	0.77	---	0.96
			STARE dataset			
			---	0.74	---	0.96
[134]		***Network architecture:*** The R2U-Net ***Approach:*** RCLs and RCLs with residual units ***Dataset:*** DRIVE, STARE, and CHASE_DB1	***DRIVE dataset***			
			---	0.78	0.98	0.95
			STARE dataset			
			---	0.82	0.99	0.97
			CHASE_DB1 dataset			
			---	0.77	0.98	0.96
[135]		***Network architecture:*** The KiU-Net Model ***Approach:*** Up-sampling layer after every conv layer in the encoder ***Dataset:*** RITE	0.75	---	---	---
[136]		***Network architecture:*** The DeepVessel network ***Approach:*** The CNN and CRF layers ***Dataset:*** DRIVE, STARE, and CHASE_DB1	***DRIVE dataset***			
			0.76	---	---	0.95
			STARE dataset			
			---	0.74	---	0.95
			CHASE_DB1 dataset			
			---	0.71	---	0.94
[137]		***Network architecture:*** The joint-loss DL framework ***Approach:*** A segment-level loss to measure the thickness inconsistency of vessel ***Dataset:*** DRIVE, STARE, CHASE DB1, and HRF	***DRIVE dataset***			
			---	0.76	0.98	0.95
			STARE dataset			
			---	0.75	0.98	0.96
			CHASE_DB1 dataset			
			---	0.76	0.98	0.96
			HRF dataset			
			---	0.78	0.96	0.94
[138]		***Network architecture:*** The AlexNet ***Approach:*** Layers of the feature hierarchy + the spatial precision of the output ***Dataset:*** DRIVE, STARE, and CHASE_DB1	***DRIVE dataset***			
			---	0.75	0.98	0.96
			STARE dataset			
			---	0.83	*0.98*	0.97
			CHASE_DB1 dataset			
			---	0.86	0.97	0.96
		Network architecture: The three-stage DL model	***DRIVE dataset***			

		Approach: ThickSegmenter, ThinSegmenter, FusionSegmenter, and pixel-wise cross-entropy loss function ***Dataset:*** DRIVE, STARE, and CHASE_DB1	---	0.98	0.95	0.76
			STARE dataset			
			---	0.98	0.96	0.77
			CHASE_DB1 dataset			
			---	0.98	0.96	0.76
[139]		***Network architecture:*** The scale-space approximated CNN (SSANet) ***Approach:*** Incorporating up-sampling layers ***Dataset:*** DRIVE, STARE, and CHASE_DB1	***DRIVE dataset***			
			---	0.83	0.97	0.95
			STARE dataset			
			---	0.85	0.99	0.97
			CHASE_DB1 dataset			
			---	0.99	0.99	0.97
[140]		***Network architecture:*** The butterfly fully convolutional neural network (BFCN) ***Approach:*** Multiscale input, dilated convolution, and the transfer layer ***Dataset:*** DRIVE, STARE, and CHASE_DB1	***DRIVE dataset***			
			---	0.81	0.98	0.96
			STARE dataset			
			---	0.82	0.99	0.97
			CHASE_DB1 dataset			
			---	0.83	0.99	0.96
[141]		***Network architecture:*** The Hard Attention Net (HAnet) ***Approach:*** Three decoder networks for regions of hard or easy and vessel segmentation ***Dataset:*** DRIVE, STARE, CHASE DB1, HRF, IOSTAR, RC-SLO, and a self-collected ICG angiography	***DRIVE dataset***			
			---	0.79	0.98	0.95
			STARE dataset			
			---	0.81	0.98	0.96
			CHASE_DB1 dataset			
			---	0.82	0.98	0.96
			HRF dataset			
			---	0.78	0.98	0.96
			IOSTAR dataset			
			---	0.75	0.99	0.96
			RC-SLO dataset			
			---	0.86	0.98	0.96
			ICG angiography dataset			
			---	0.87	0.98	0.96
[142]		***Network architecture:*** The Deep Residual Learning ***Approach:*** Wide Activation (WA-Net) + LASPP module ***Dataset:*** DRIVE and STARE	***DRIVE dataset***			
			---	0.78	0.98	0.95
			STARE dataset			
			---	0.77	0.99	0.96
[143]		***Network architecture:*** The Contextual Multi-Scale Multi-Level Network ***Approach:*** Fusing the global contextual features of multiple spatial scales + re-exploiting the dilated convolution module ***Dataset:*** DRIVE	0.80	0.78	0.98	0.96
[144]		***Network architecture:*** ResDO-UNet ***Approach:*** Combined with depth-wise over-parameterized convolutional layer and taking advantage of max pooling and average pooling layers, a pooling fusion block ***Dataset:*** DRIVE, STARE, and CHASE DB1	***DRIVE dataset***			
			---	0.79	0.97	0.95
			STARE dataset			
			---	0.80	0.98	0.96
			CHASE_DB1 dataset			
			---	0.80	0.97	0.96
[145]	Abdominal / CT and CTA	***Network architecture:*** The U-Net ***Approach:*** 2D patch-based segmentation and area imbalance reduced training patch generation (AIRTPG) ***Dataset:*** 20 cases of abdominal	---	0.88	---	---
[146]		***Network architecture:*** CNN ***Approach:*** Hough Circles Algorithm ***Dataset:*** CT and CTA images of ten patients	---	0.98	---	0.98
[147]	Coronary vessels / X-ray	***Network architecture:*** The U-Net ***Approach:*** The DenseNet121 ***Dataset:*** X-ray coronary angiography images of 2042 patients	---	0.92 ± 0.11	---	---
[148]	Head and Neck Vessels / CTA	***Network architecture:*** The 3D-CNN model ***Approach:*** The bottleneck-ResNet (BR) + ResU-Net + connected growth prediction model (CGPM) ***Dataset:*** 18,766 head and neck CTA scans	0.94	0.93	---	0.93

Table 5. Summary of DL approaches in pathology image segmentation.

Ref	Organ/ modality	Method	Performance metrics			
			DSC	***TPR***	***TNR***	***ACC***
[149]	Breast and colon cancer	***Network arch:*** DCNN ***Approach:*** Extracted descriptors with CNN and PiCoDes ***Dataset:*** NA	---	0.83	0.84	---
[150]	Breast and colon cancer	***Network arch:*** DCNN ***Approach:*** Feature extraction with DCNN ***Dataset:*** NA	---	0.87	0.82	0.85
[151]	Brain/needle-core biopsy	***Network arch:*** U-Net ***Approach:*** Multiclass segmentation with periodic acid–Schiff (PAS) with CNN ***Dataset:*** NA	0.87	---	---	---
[152]	Mitosis in a histopathological tissue	***Network arch:*** U-Net/ AlexNet ***Approach:*** Classify and detect mitosis using U-Net and AlexNet ***Dataset:*** NA	0.6	0.94	0.95	0.95
[153]	Brain MRI and pathology images	***Network arch:*** U-Net ***Approach:*** Used U-Net and AlexNet, then outputs feed into ResNet-101 ***Dataset:*** NA	---	---	---	0.90
[154]	Shoulder muscle MRI	***Network arch:*** U-Net ***Approach:*** Categorize adult diffuse glioma cases into oligodendroglioma and astrocytoma classes using radiographic and histologic image data using DL ***Dataset:*** NA	0.93	0.78	0.38	---
[155]	Cervical cancer tissue	***Network arch:*** AF-SENet ***Approach:*** Fine-tuning pre-trained DNNs/ classification AF-SENet ***Dataset:*** NA	---	---	---	0.95
[122]	Liver cancer histopathology images	***Network arch:*** U-Net ***Approach:*** Using a robust residual block, a bottleneck block, and an attention decoder block ***Dataset:*** KMC dataset/ Kumar dataset	0.68	---	---	---
[156]	Liver cancer/ colon cancer/ g breast cancer metastases histopathology images	***Network arch:*** DenseNet-121, Inception-ResNet-V2, and DeeplabV3Plus ***Approach:*** Sequence of individual techniques in the preprocessing training-inference pipeline ***Dataset:*** CAMELYON16, CAMELYON17	0.78	---	---	---
[157]	Pathological Myopia / retinal images	***Network arch:*** CNN ***Approach:*** CNN bundles lesion segmentation and PM classification ***Dataset:*** Pathological Myopia (PALM) dataset	0.93	---	---	---
[158]	Renal pathology images	***Network arch:*** D***y***namic single segmentation network (Omni-Seg) ***Approach:*** Omni-Seg learns to segment multiple tissue types using partially labeled images ***Dataset:*** NA	0.96	---	---	---

Biographies:

Mahdiyeh Rahmani is a Ph.D. candidate in Biomedical Engineering at Tehran University of Medical Sciences, Tehran, Iran. She has actively contributed to the field of medical image processing as a research assistant at the Image Guided Surgery Lab at the Research Center for Biomedical Technology & Robotics in Tehran, Iran. Her research is centered at the intersection of Biomedical Engineering and Computer Science, with a particular focus on advancing the frontiers of healthcare through innovative applications of Medical Image Processing and Deep Learning technologies.

Ali Kazemi is a Ph.D. candidate in Biomedical Engineering (Bioelectric) at the Tehran University of Medical Sciences. He received an M.Sc. degree in Biomedical Engineering (Bioelectric) from Tabriz University of Medical Sciences in 2020 and a B.Sc. degree in Biomedical Engineering (Bioelectric)

from the Science and Research Branch, Islamic Azad University in 2016. His research interests include Biomedical Image Processing, Machine Learning, and Deep Learning.

Maryam Jalili Aziz received a B.Sc. degree in Biomedical Engineering from the University of Isfahan, Isfahan, Iran, in 2016 and an M.Sc. degree in Biomedical Engineering from Tehran University of Medical Sciences, Tehran, Iran, in 2021. She is currently pursuing a Ph.D. degree in Engineering Science with the Department of Electronics and Informatics, Vrije Universiteit Brussel (VUB), Brussels, Belgium.

Ebrahim Najafzadeh received his Ph.D. degree in medical physics in 2020 from Tehran University of Medical Sciences, Iran. He is an assistant professor at the Department of Medical Physics, School of Medicine at Iran University of Medical Sciences, Iran. His research interests include artificial intelligence, medical imaging, Photoacoustic, and Fluorescence Molecular Imaging.

Parastoo Farnia received her Ph.D. degree in Biomedical Engineering, in 2020, from Tehran University of Medical Sciences, Iran. She is an Assistant Professor at the Department of Medical Physics and Biomedical Engineering, Faculty of Medicine at Tehran University of Medical Sciences, Iran. Her research interests include Medical Image processing, Image Registration, Machine learning, and Deep learning.

Alireza Ahmadian received his Ph.D. degree in Biomedical Image Processing, in 1997, from Imperial College of Science and Technology in Medicine, London, UK. He is a professor at the Department of Medical Physics and Biomedical Engineering, Faculty of Medicine at Tehran University of Medical Sciences, Iran. Also, He is head of the Research Center for Biomedical Technology & Robotics, RCBTR, Tehran, Iran. His research interests include Image-guided surgery Systems, Biomedical Signal Processing, and Medical Image registration.